

FILE COPY
NO. I-W

ACR Feb. 1943

NATIONAL ADVISORY COMMITTEE FOR AERONAUTICS

WARTIME REPORT

ORIGINALLY ISSUED

February 1943 as
Advance Confidential Report

DEVELOPMENT OF THERMAL ICE-PREVENTION EQUIPMENT

FOR THE B-24D AIRPLANE

By Alun R. Jones and Lewis A. Rodert

Ames Aeronautical Laboratory
Moffett Field, California

FILE COPY
To be returned to
the files of the National
Advisory Committee
for Aeronautics
Washington, D. C.



WASHINGTON

NACA WARTIME REPORTS are reprints of papers originally issued to provide rapid distribution of advance research results to an authorized group requiring them for the war effort. They were previously held under a security status but are now unclassified. Some of these reports were not technically edited. All have been reproduced without change in order to expedite general distribution.

NATIONAL ADVISORY COMMITTEE FOR AERONAUTICS

ADVANCE CONFIDENTIAL REPORT

DEVELOPMENT OF THERMAL ICE-PREVENTION EQUIPMENT
FOR THE B-24D AIRPLANE

By Alun R. Jones and Lewis A. Rodert

SUMMARY

A thermal ice-prevention system for the B-24D airplane has been developed at the Ames Aeronautical Laboratory of the National Advisory Committee for Aeronautics in cooperation with the Materiel Center of the Army Air Forces and the Consolidated Aircraft Company. The subject report includes a description of the design and an outline of the method of design analysis. Results of performance tests of the installation are to be presented in a supplementary report.

The thermal ice-prevention system is based upon raising the temperature of the surfaces to be protected from ice formations by subjecting the inner face of the surface to a stream of heated air. The sources of heated air are four exhaust gas-air heat exchangers, one on each engine. A double-skin type of construction was employed for the wings and tail surfaces, and double-pane construction for the windshields. The heated air is caused to circulate by the dynamic pressure of the air stream.

A design analysis is presented in a general form, as a possible outline for future computations, and is illustrated with sample calculations from the B-24D airplane analysis.

INTRODUCTION

In cooperation with the Materiel Center of the Army Air Forces, the Consolidated Aircraft Company, and several equipment manufacturing companies, the Ames Aeronautical Laboratory has designed, installed, and tested in flight thermal ice-prevention equipment on the B-24D airplane. The work was undertaken at the request of the Materiel Center in order to relieve the aviation industry

of some of the design and development work which is required in the introduction and application of the thermal method of ice prevention. It was desired that the equipment be developed so that production could be undertaken at once by the airplane manufacturer. Attention, therefore, was given in the design to service, weight, production possibilities, and other such features. Mr. Howard F. Schmidt, Consolidated Aircraft Company representative at AAL for this project, contributed materially in the development.

The rapidity with which the project was undertaken and completed was due to the interest and cooperation given by all of the interested agencies.

DESCRIPTION OF THE ICE-PREVENTION EQUIPMENT

The B-24D airplane is shown in figure 1. The airplane is a high-wing, tricycle-gear, heavy bomber powered by four Pratt & Whitney S3C4G engines, rated at 1100 horsepower. An exhaust-gas-driven engine supercharger is located in each nacelle.

The general layout of the heated-air anti-icing system designed for the B-24D airplane is shown in figure 2. Heated air is obtained from an exhaust gas-air heat exchanger in each nacelle. After passing through the exchanger, the air is directed to the various regions to be heated by a system of thin-wall ducts. The dynamic pressure of the air stream augmented by the propeller provides the source of energy for the circulation of the heated air.

The design of the thermal ice-prevention equipment for the wing outer-panel leading edge (stations 335 to 626, fig. 2) is shown in figure 3. A spanwise duct is formed in the wing structure by placing a baffle at 4.5 percent of the wing chord, and the heated air from the outboard heat exchangers is carried to this spanwise duct by the four-branch pipe system shown in figure 2. The corrugated inner skin and the outer skin form a series of chordwise passages for the heated air. The air enters the passages through a gap in the corrugations at the wing leading edge and flows along the top and bottom inner surfaces of the outer skin to the termination of the corrugations at the front spar (fig. 4). A series of reinforced holes in the front and rear spar webs allows the air to

pass through the wing interior and out into the aileron slot region. The outer panel leading edge, ready for installation on the airplane, is shown in figure 5.

At the wing tip (fig. 6) the air, after having passed through the leading-edge system of the wing outer panel, is allowed to pass into the forward portion of the tip and is then made to flow between the outer and inner skins. All of the wing-tip heated air leaves the wing on the upper surface, in front of the navigation light.

The thermal ice-prevention equipment design for the wing inboard-panel leading edge (stations 164 to 275) is shown in figure 7. A portion of the heated air at each inboard exchanger outlet is diverted to the inboard-panel leading edge, as shown in figure 2. The air enters a triangular-section spanwise duct located at the front-spar lower flange, which runs the entire length of the inboard panel. The air is allowed to enter the chordwise passages, formed between the outer skin and an inner corrugated skin which is continuous around the leading edge, through a small gap at the bottom of the triangular duct. The corrugation passages are sealed at their upper ends and the air passes into the outside boundary layer through 1/2-inch-diameter holes in the outer skin. Circulation of the heated air inside the wing is normally desirable, but was not feasible in the case of the inboard panel because of the wheel-well cut-out in the lower skin. The inboard-panel leading edge during installation on the airplane is shown in figure 8.

In addition to supplying the inboard wing panels, the inboard heat exchangers also furnish air for the empennage group and windshields. The duct system in the wings and fuselage is shown in figure 2.

The thermal ice-prevention equipment design for the empennage group is shown in figure 9. The heated air is passed through a 4-inch-diameter tube mounted spanwise in the stabilizer leading edge. (See fig. 10.) A small slot was cut in the duct between stabilizer ribs and the thin duct wall bent inward to form a scoop as shown in the slot detail of figure 9. A second skin was attached around the stabilizer leading edge, extending 12 inches from the leading edge on the top and bottom surfaces. Chordwise spacers were employed to maintain a constant gap of about 0.051 inch between the two leading-edge skins. All lightning holes in the front spar were sealed with metal plates. A portion of the heated air in the spanwise supply duct passes

through the scoop slots in the duct, through holes in the leading edge of the inner skin, between the two skins in a chordwise direction, and over the upper and lower surfaces of the stabilizer behind the front spar. The quantity of heated air remaining in the supply duct is discharged from the duct at the stabilizer tip and passes through holes in the inboard skin of the fin into the fin plenum chamber.

The fin plenum chamber is a sealed region, formed by placing baffles between the webs of the fin ribs, and provides a practical method for passing the heated air from the stabilizer to the fin. The plenum chamber is shown in figure 11. The fin thermal ice-prevention equipment design is similar to that of the stabilizer. A second skin was wrapped around the leading edge to a distance of 9 inches from the leading edge, and spacers were employed to provide a constant gap between skins of 0.0625 inch. Two 3-inch flexible ducts with outlets at the ends only were fastened to the plenum chamber to direct the air to the top and bottom of the fin. Lightning holes in the front spar and the two end ribs (see fig. 9) were sealed in order to retain all of the heated air in the leading-edge region and force it through the double-skin gap. The empennage group, revised for thermal ice-prevention and installed on the airplane, is shown in figure 12.

The thermal ice-prevention equipment for the windshields is shown in figure 13. Protection is provided for both the pilot's and the copilot's windshields, and the heated-air-supply ducting is shown in figure 2. The windshield design consists of an inner Plexiglas panel, readily removable in flight and spaced uniformly $1/8$ inch from the outer panel, and an entrance and exit header for the heated air. The heated air flows spanwise across the windshield, from the inboard edge outward, and exhausts from the exit header to the outside air stream through slots cut into the forward edge of the side window.

The exhaust gas-air heat exchangers were designed around an existing portion of the exhaust-gas tail-stack located on the bottom of each nacelle between the collector ring and the turbosupercharger. Several heat exchangers of the extended surface type (having pins or fins protruding into both the exhaust-gas and heated-air regions) have been tested on the airplane. Figure 16 shows one of the types tested.

In addition to the finned tube, the heat exchanger

consists of an aluminum intake scoop (opening, 3 by 6 in.), a stainless-steel shroud around the finned region, and an outlet manifold. The outlet of each inboard heat exchanger includes a right-angle bypass, with a butterfly valve, for the purpose of supplying and controlling heated air to the wing inboard panels. One of the heat exchangers is shown installed in the airplane in figure 17.

Control of the thermal ice-prevention system was accomplished by locating an electric motor-operated dump valve in each nacelle near the heat-exchanger outlet. (See fig. 18.) The operating mechanisms for the inboard dump valves were extended to include the butterfly valves in the inboard-panel supply ducts. The controls for each nacelle are independent; they are located within reach of the copilot and are connected in such a manner that the dump valves are always either fully open or fully closed. The distribution of heated air in the wing outer-panel supply ducts can be varied by means of three butterfly valves in each wing, located in the three inboard (stations 368, 450, and 515) heated-air supply ducts near the front spar. These valves are adjustable when the airplane is on the ground. The quantity of air directed to the windshields is controlled by a butterfly valve in the single supply line running forward in the fuselage. This valve is normally in a fixed position, but it is accessible to crew members. There are no valves in the empennage heated-air supply lines other than the inboard-nacelle dump valves.

DESIGN ANALYSIS FOR THERMAL ICE-PREVENTION EQUIPMENT

A design analysis of the thermal ice-prevention equipment was prepared to establish the dimensions of the heated air passages and ducts required to produce the desired temperature, air-flow distributions, and pressure drops. The general procedure followed in the analysis is outlined in the following pages, with the various steps numbered. A brief discussion of the pertinent data associated with each step is presented, and actual computations from the B-24D airplane calculations are presented as examples.

The following notation was used in the analysis:

- A cross-sectional area, square feet
- S surface area, square feet

Q	total heat flow, Btu per hour
q	unit heat flow, Btu per hour per unit length of span
h	surface heat-transfer coefficient, Btu per hour, square feet, $^{\circ}\text{F}$
t	temperature, $^{\circ}\text{F}$
T	temperature, $^{\circ}\text{F}$ absolute
W	weight rate of air flow, pounds per hour
w	unit weight rate of air flow, pounds per hour per unit length of span
c_p	specific heat of air, Btu per pound, $^{\circ}\text{F}$
μ	absolute viscosity of air, pounds per second, feet
k	thermal conductivity of air, Btu per hour, square feet, $^{\circ}\text{F}$ per foot
G	weight rate of air flow per unit of cross-sectional area, pounds per second, square feet
P	static pressure, pounds per square foot
d	thickness of gap between surfaces, feet
N	length of air passage or duct, feet
m	hydraulic radius, or ratio of cross-sectional area to wetted perimeter in a duct, feet
D_e	equivalent diameter of a duct, equal to $4m$, feet
v	specific volume, cubic feet per pound
R	gas constant (53.3 for air)
g	acceleration of gravity, feet per second ²
f	friction coefficient for air flow in ducts
s	distance as measured around wing leading edge, feet
V	airplane indicated airspeed, miles per hour
c	chord, feet

Subscripts:

av refers to average conditions

1, 2, 3, etc. are employed to define surfaces or air spaces and used as subscripts to indicate temperature differences, heat flow, and heat-transfer coefficients. Thus the heat-transfer coefficient between a given surface (6) and adjacent air (2) would be written h_{e-2} .

A few symbols used in the analysis are not presented in the notation because they do not appear throughout the calculations and because their meaning is much clearer if defined at the place of their use.

The analysis was based on an assumed airplane indicated airspeed of 150 miles per hour at 18,000-foot pressure altitude.

Step 1. Assumption of free-air temperature.- Most cases of aircraft icing occur between the temperatures of 0° and 32° F. For the B-24D airplane analysis the value of 0° F was assumed.

Step 2. Assumption of average temperature at which the heated surface is to be maintained.- According to reference 2, paragraph D-6b, the temperature rise over the forward 25 percent of the wing chord must be at least 70° F above ambient air, and the rise between 25 and 75 percent of the chord must be at least 20° F above ambient air. Direct heating of the leading edge for 25 percent of the chord is difficult to obtain in certain designs, and in such cases the assumption is made that by heating directly a smaller portion of the leading edge (say 10 to 15 percent) to a temperature rise of 100° F (instead of 70° F) and then discharging the heated air to the remainder of the wing, the specifications of reference 2 can be satisfied. The Lockheed 12A of reference 1 is an example of this compromise in design which has proved capable of providing ice prevention. Direct heating was provided for the forward 12 percent of the wing, raising the wing temperature approximately 100° F, and the heated air was discharged from the leading-edge region and circulated through the remainder of the wing.

Direct heating of the B-24D airplane wing was limited to the forward 10 percent because the location of the front

spar at that point prohibited further extension of the corrugated inner skin. The corrugated region of the skin was subject to thermal analytical treatment. The heated-wing design was based upon a 100° F temperature rise over the forward 10-percent-chord region and an indeterminate temperature rise over the remainder of the wing. A temperature rise of the wing after-portion will occur because of the heated boundary layer, and the discharge air from the leading-edge system. In the case of the wing outer panel, the heated air was discharged through the front spar and circulated in the wing interior, similar to the Lockheed 12A airplane design. For the inboard panel, however, the heated air could not be circulated in the wing interior. The heated air was therefore released to the boundary layer on the upper surface and carried back over the wing. The stabilizer and the fin were treated in a manner similar to the wing inboard panel, with the exception that the heated air was discharged over both surfaces of the airfoil sections. The double-skin system for the empennage was dictated by the simplicity of the revisions required on the existing empennage, and the desirability of producing a suction at the heated-air exit to aid the heated-air flow. The horizontal stabilizer leading-edge skin temperature was raised 90° F, and the fin leading-edge skin temperature was raised 70° F in the design. This heating of the empennage surfaces should be adequate because the discharged air from the leading-edge system is effectively distributed over both sides of the airfoil.

Step 3. Calculation of the heat-transfer coefficient between the wing surface and the ambient air.— With the temperature difference between the wing skin and the ambient air established, the quantity of heat removed from the wing skin depends upon the outer-surface heat-transfer coefficient. The coefficient can be calculated from the data in reference 3, although this method involves some error because of the low Reynolds number at which the tests were made. Another method of determining the heat-transfer coefficient, based upon the relation between heat transfer and viscous drag, is presented in reference 4. For the B-24D airplane analysis, the data in reference 3 were employed by extrapolating in the equation

$$h'' = h' \frac{c'}{c''} \left(\frac{V'' c''}{V' c'} \right)^n \quad (1)$$

where the first prime refers to values from reference 3, the second prime to values for the B-24D analysis, and n

is a constant dependent upon the portion of the wing chord under consideration and the angle of attack of the airfoil. The effect of changes in altitude upon the value of the heat-transfer coefficient (h) has been conservatively neglected in the derivation of equation (1). In the case of the B-24D wing outer panel, the design analysis was based upon supplying enough heat to the wing forward of the front spar to produce the 100° F rise of step 2. The value of n for equation (1), therefore, was obtained from table I, reference 3, corresponding to the forward section of an airfoil at approximately 2° angle of attack. The design indicated airspeed ($V'' = 150$ mph) and the various values of outer-panel chord (c'') were substituted in equation (1) to produce the values of h plotted in figure 19. The subscripts employed in figure 19 are used in the manner explained under Notation and refer to the regions and surfaces shown in section A-A, figure 20.

Step 4. Calculation of the total heat flow from the critical design surface. - In order to estimate the quantity of heat that must be supplied to the thermal ice-prevention system to produce the required temperature rise, the total heat flow from the design critical surface must be calculated by equation

$$Q_{6-7} = (h_{6-7})_{av} S(t_{6-7})_{av} \quad (2)$$

(See equation (1), p. 136, reference 5.) For the B-24D airplane-wing outer panel, the design surface was the entire outer-panel surface forward of the front spar. The distance around the wing leading edge from top to bottom of the front spar is shown in figure 19, and the average value for the outer panel multiplied by the panel span resulted in a surface area of 45.3 square feet. From figure 19, h_{av} for the outer panel = 13 Btu per hour, square feet, $^{\circ}$ F. Then

$$Q_{6-7} = 13 \times 45.3 \times 100 = 59,000 \text{ Btu per hour}$$

Step 5. Estimation of the amount of heat that should be available in the heated air to insure the necessary heat flow to the surface. - The quantity of heat that must be supplied to the design surface is taken to be from two to four times the heat flow from that surface, depending upon the amount of heating the air is expected to deliver after leaving the leading-edge region. In the B-24D outer

panel the total heat to be supplied to the leading-edge region was assumed to be 200,000 Btu per hour.

Step 6. Assumption of a temperature rise for the heated air in passing through the heat exchanger. - The design temperature rise through the heat exchanger is usually determined by the maximum temperature allowable for the heat exchanger and heated-air-duct materials, and possible effects of elevated temperatures on the airplane primary structure. A heated-air temperature of 300° F at the exchanger outlet was considered to be a reasonable and safe design value for the B-24D airplane.

Step 7. Calculation of the rate weight of air flow required. - The quantity of air that must pass through the heat exchanger in a given time, with a temperature rise established by step 6 in order to produce the available heating of step 5, is determined by

$$W = \frac{Q}{c_p \Delta t} \quad (3)$$

where Δt is the heated-air temperature rise in °F. For the B-24D outboard heat exchangers using the value of c_p from figure 21,

$$W = \frac{200000}{0.24 \times 300} = 2730 \text{ pounds per hour}$$

Step 8. Design of the heated air passages. - The design procedure employed was to divide the wing surface into unit strips running chordwise and consider the heat flow for a sufficient number of strips to define the wing heating. The width of the division strips for the outer wing panel was taken as 1 inch, or the spanwise distance covered by a single corrugation.

Step 9. Application of steps 2, 3, and 4 to individual chordwise strips. - The heat flow from the outer-surface area of each strip considered is determined by application of steps 2, 3, and 4 in the same manner as employed to determine the total heat flow from the total critical surface. The single corrugation strip at the inboard edge of the outer wing panel (station 335) will serve as an example. The heat flow from the outer surface,

$$q_{6-7} = h_{6-7} t_{6-7} \frac{s}{12} \quad (4)$$

$$h_{6-7} = 11.6 \text{ Btu per hour, square feet, } ^\circ\text{F} \quad (\text{fig. 19})$$

$$s = 2.45 \text{ feet} \quad (\text{fig. 19})$$

$$t_{6-7} = 100^\circ \text{ F} \quad (\text{step 2})$$

$$q_{6-7} = 11.6 \times 100 \times \frac{2.45}{12} = 237 \text{ Btu per hour}$$

Step 10. Assumption of weight distribution of heated air.— The distribution of the heated air to the various air passages is determined by trial and error, consideration being given to such factors as the larger heating requirement at the wing root, the increased surface transfer coefficient at the wing tip, and the pressure drop in the air ducts and passages. The final weight distribution which proved satisfactory in the airplane analysis was to supply the air to the corrugations in quantities inversely proportional to the square root of the distance around the leading edge, or

$$w = w_{av} \sqrt{\frac{s_{av}}{s}} \quad (5)$$

The B-24D airplane-wing outer panel has 291 corrugations; therefore the value of w at station 335,

$$w = \frac{2730}{2 \times 291} \sqrt{\frac{1.87}{2.45}} = 4.1 \text{ pounds per hour}$$

Step 11. Calculation of the temperature drop of the heated air in the chordwise passages.— The quantity of air flowing in each passage and the heat removed from the air having been established, the temperature drop of the heated air can be calculated by applying an adaptation of equation (3). For the corrugation at station 335,

$$t_1 - t_3 = \frac{q_{6-7}}{2 c_p w} = \frac{237}{2 \times 0.24 \times 4.1} = 118^\circ \text{ F}$$

Step 12. Design of the heated air passage to produce the required heat flow.— The remaining step is to vary the

Reynolds number of the heated air by changing the air-passage dimensions until a heat-transfer coefficient for the inside of the passage is produced which will supply the necessary heat to the outer skin, with the average temperature of the air in the passage determined from step 11. The Reynolds number for the flow of the heated air is expressed:

$$Re = \frac{G D_e}{\mu} \quad (\text{See pp. 99 and 235, reference 5.})$$

The heat-transfer coefficient for the inner surface of the passage is determined from empirical data showing the variation of the Nusselt number with Reynolds number where the Nusselt number

$$Nu = \frac{h D_e}{k} \quad (\text{See p. 96, reference 5.})$$

Empirical data which have proven satisfactory in determining the air-passage heat-transfer coefficient are presented in figure 65, reference 5, and the recommended curve AA from the figure has been reproduced in figure 22. The data determining the curve AA in figure 22 are directly concerned with fluid flow in circular ducts, but experience has shown that reasonably accurate calculations for ducts of noncircular cross section can be based upon the curve AA, provided the departure from a circular cross section is not too severe. In designs where the air passage consists of two parallel plates, such as the empennage and windshield design for the present airplane, the empirical data presented in figure 7 of reference 6 and reproduced in figure 22 are recommended. These data are plotted on the basis of the gap width d as the equivalent diameter D_e , and their comparison in figure 22 with the recommended curve AA from reference 5 reveals the error that can be introduced by applying curve AA to air passages of noncircular section.

In the case of the B-24D airplane wings, the heat-transfer coefficient inside the corrugation air passages was based upon curve AA, figure 22. Considering the single corrugation at station 335,

$$G = \frac{w}{3600 A} = \frac{4.1}{3600 \times 0.000765} = 1.49 \text{ pounds per second, square foot}$$

The hydraulic radius of the air passage (see corrugation detail in fig. 3) is equal to 0.0043 foot. With the value of μ from figure 21,

$$Re = \frac{G D_0}{\mu} = \frac{1.49 \times 4 \times 0.0043 \times 10^5}{1.5} = 1710$$

From curve AA, figure 22, for $Re = 1710$,

$$Nu = \frac{h_{2-6} D_0}{k} = 7.6$$

From figure 21, $k = 0.0162$, and therefore,

$$h_{2-6} = \frac{7.6 \times 0.0162}{4 \times 0.0043} = 7.3 \text{ Btu per hour, square feet, } ^\circ\text{F}$$

The average temperature of the air in region 2, assuming $t_1 = 300^\circ\text{F}$,

$$t_{2\text{av}} = 300 - \frac{118}{2} = 241^\circ\text{F}$$

The quantity of heat flow to the skin then becomes

$$q_{2-6} = h_{2-6} \times \frac{s}{12} \times (t_{2\text{av}} - t_6)$$

$$= 7.3 \times \frac{2.45}{12} \times 141$$

$$= 210 \text{ Btu per hour}$$

This value of q_{2-6} is in satisfactory agreement with the value of q_{6-7} equal to 237 Btu per hour determined in step 9. The thermal design for the wing inboard panel and the empennage was made in a manner similar to that used for the outboard-panel design, and the results are shown in figures 20 and 23.

In the case of the B-24D airplane windshield, sufficient data were not available to determine the heat-transfer coefficient from the outer surface. Steps 2, 3, and 4 of the design procedure were replaced by the assumption that a heat flow from the outer surface of 1000 Btu

per hour, square feet would be sufficient to provide ice protection. (See p. 8, reference 1.) Further necessary assumptions were the temperature of the windshield outer panel, assumed to be 50° F, and the temperature of the air entering the gap between the panels, assumed to be 150° F. The design was then completed by assuming different quantities of air flow and values of gap size until a combination was found which would produce the required outer-panel heating. The results of the windshield analysis are shown in figure 20. The desired temperature rise for the critical surfaces having been established, the pressure drop in the air passages and the design of the heated air-supply ducts to obtain the necessary weight of flow distribution are examined. Unless an air pump of some sort is incorporated in the thermal anti-icing system, the circulation of the heated air is dependent upon the total energy of the air at the heat-exchanger inlet. Secondary factors which may be considered to aid the propulsion of the air through the system are the addition of energy to the air in passing through the heat exchanger and the location of the air outlet at a point of low pressure. For the B-24D thermal ice-prevention system, the energy effect in the heat exchanger was neglected and a pressure drop of 5 inches of water, or approximately one-half the value of the dynamic pressure for the design indicated speed of 150 miles per hour, was assigned to the heat exchangers. In order to obtain the weight distribution of air desired in the surface-heating calculations, the pressure drop must be equal along all heated air paths, from the heat-exchanger outlet to the air exit from the wing. The general design procedure is to calculate the pressure drop required in the various air passages and then design the supply ducts to produce equal pressure drop in all of the possible air paths.

The pressure drop in the heated air passages and the supply ducts was calculated by the equation

$$P_1 - P_2 = \frac{G^2 (v_2 - v_1)}{g} + \frac{f_{av} N G^2 v_{av}}{2 g m} \quad (6)$$

(equation (35), p. 130, reference 5), where the subscripts 1 and 2 represent the extent of region over which the pressure drop is calculated. The first term of equation (6) was found to be negligible in this case and therefore dropped from the equation. Data from which the friction factor f_{av} may be obtained are presented in figure

24, which is a reproduction of figure 8, reference 6. The curve in figure 24 refers to flow in circular pipes, and the data plotted in the figure were obtained in model tests with air flow in a narrow gap between parallel surfaces. Figure 24 was employed in the analysis in the same manner as figure 22; that is, the curve for circular pipes was used when determining f for the corrugated air passages and supply ducts, and the plotted data were used when determining f for air flow in the empennage and windshield gaps.

Considering a single corrugation air passage at station 335, outer wing panel,

$$v_{av} = \frac{RT}{P} = \frac{53.3 \times 701 \times 2}{2116} = 35.4 \text{ cubic feet per pound}$$

The static pressure at 18,000 feet was used in calculating the specific volume.

$$Re = \frac{G D_e}{\mu} = \frac{1.49 \times 4 \times 0.0043 \times 10^5}{1.5} = 1710$$

$$f_{av} = 0.0094 \quad (\text{from curve in fig. 24})$$

$$n = \frac{s}{2} = 1.22 \text{ feet}$$

$$G = \frac{w}{3600 A} = \frac{4.1}{3600 \times 0.000765} = 1.49 \text{ pounds per second, square foot}$$

$$m = 0.0043 \text{ feet}$$

Pressure drop from region 1 to region 3,

$$P_1 - P_3 = \frac{f_{av} N G^2 v_{av}}{2 \text{ gm}} = \frac{0.0094 \times 1.22 \times 1.49^2 \times 35.4}{2 \times 32.2 \times 0.0043}$$

$$P_1 - P_3 = 3.3 \text{ pounds per square foot} \quad \text{or} \quad 0.6 \text{ inch of water.}$$

Extension of the pressure-drop calculations to other corrugation air passages in the wing outer panel indicated that the pressure drop from region 1 to region 3 was substantially constant for the entire panel. (See sec. AA,

fig. 20.) In order to produce the desired distribution of the heated air, therefore, the pressure drop from the outboard heat-exchanger outlet to any point in region 1 had to be constant. The spanwise pressure drop along region 1 was found to be too large if all of the heated air were admitted to the region at station 335, hence the air was supplied in four tubes as shown in figure 2. The pressure drop through the corrugation passages in the inboard-panel leading edge was calculated to be 5 inches of water as shown in section BB, figure 20. This large drop was considered allowable because of the location of the heated-air-exit holes in a low-pressure region. For the empennage group (fig. 23) the fin heated-air gap was designed larger than the stabilizer gap in order to approximately compensate for the pressure drop in the stabilizer leading-edge supply duct.

Instrumentation of the B-24D Airplane for Tests

Thermocouples, pressure orifices, and venturi meters were included in the design of a portion of the B-24D airplane thermal ice-prevention equipment in order to measure the performance of the installation in flight tests. The following factors were considered to be of interest:

1. Quantity of air flow through the heat exchangers and various parts of the equipment.
2. Temperature of the heated air throughout the system.
3. Temperatures of heated surfaces, namely, wing and empennage outer surfaces, parts of the internal structure, windshield panels, and heat-exchanger surfaces.
4. Temperature of the exhaust gas.
5. Static and total pressure at the heat-exchanger inlets, and static pressure of the heated air throughout the system.
6. Exhaust-gas static-pressure drop through the heat exchanger.

The quantity of air flow was determined by the use of

venturi meters. Four such meters were installed, as shown in figure 2: one in the 5-inch supply line from the right outboard heat exchanger, one in the 3-inch inboard-panel supply line from the right inboard heat exchanger, one in the 2-inch supply duct to the copilot's windshield, and one in the 6-inch supply duct to the empennage (located aft of the junction of the ducts from the inboard heat exchangers). The ratio of the throat diameter to pipe diameter for the venturi meters was 0.7.

All temperature readings were obtained with iron-constantan thermocouples and a Lewis potentiometer. The identification drawing for the thermocouples is shown in figure 25. The dash numbers following the thermocouple numbers in figure 25 refer to the type of thermocouple mounting, as detailed in figure 26. The Plexiglas shield for type 5, figure 26, was required because the thermocouple junction otherwise would move away from the outer skin and protrude into the ambient air stream. Two thermocouples were located in the intake scoop of the right inboard heat exchanger.

The locations of the pressure-measurement points are shown in figure 27. All measurements were of static pressures, with the one exception of the total pressure in the intake scoop of the right inboard heat exchanger. Three total-pressure heads and two static-pressure heads were distributed across the exchanger inlet because preliminary flight tests revealed a variation in total head in that region at low angles of attack. The dash numbers following the pressure-orifice numbers in figure 27 refer to the type of orifice mounting as shown in figure 28.

All pressures, with the exception of the exhaust-gas pressures, were referred to the total pressure from the pitot-static airspeed heads located at the nose of the airplane. The pressure differentials were indicated by water manometers and airspeed indicators. The absolute values of the two exhaust-gas pressures were indicated by a manifold pressure gage. A calibration of the difference between the static pressure at the airplane airspeed heads and free-stream static pressure was obtained by suspending a trailing static head from the airplane. The static calibration of the airspeed heads provided a basis for referring the test pressures to free-stream static pressure and for determining the correct indicated airspeed of the airplane.

PRELIMINARY FLIGHT TESTS - RESULTS AND DISCUSSION

Preliminary flights have been conducted with the B-24D airplane to test the performance of the thermal ice-prevention equipment. Supplying a quantity of heat to the wing outer panel equal to approximately 65 percent of the design quantity produced a temperature rise of the skin forward of the front spar slightly in excess of the design value. Indications are that the remainder of the thermal ice-prevention design will be equally satisfactory when heat quantities approximating the design values are supplied from all four heat exchangers. Data on the performance tests of the complete installation will be presented as a supplementary report later.

Weight of Equipment

Calculations have been made to estimate the increase in weight of a B-24 airplane resulting from the installation of a production modification of the subject thermal ice-prevention system. A study of a production design was considered more desirable than a presentation of the weights of the B-24D airplane installation because that installation is an experimental revision to an existing airplane and the weight factor was not given the consideration that it would receive in a production design. The calculations indicated that the weight of a B-24 airplane (not equipped for ice protection) would be increased about 300 pounds by the installation of thermal ice-prevention equipment. Attention is called to the fact that the figure of 300 pounds is subject to revision on the basis of maintenance and durability requirements as determined by the manufacturer's experience. The 300-pound weight of the present equipment compares with the 230-pound weight of the inflatable de-icer equipment that it replaces. The latter does not include windshield de-icing, however.

CONCLUSIONS

1. Thermal ice-prevention equipment for the B-24D airplane wings, empennage, and windshield is structurally feasible.
2. The thermal ice-prevention equipment installation will probably satisfy all design requirements.

3. A modified production installation of the thermal ice-prevention system would increase the weight of a B-24 airplane (not equipped for ice protection) about 300 pounds.

Ames Aeronautical Laboratory,
National Advisory Committee for Aeronautics,
Moffett Field, Calif.

REFERENCES

1. Rodert, Lewis A., Clousing, Lawrence A., and McAvoy, William H.: Recent Flight Research on Ice Prevention. NACA A.R.R., January 1942.
2. Army Air Forces Specification No. R-40395: Anti-icing Equipment for Aircraft, General Specifications (Heated Surface Type). A.A.F., April 21, 1942.
3. Theodorsen, Theodore, and Clay, William C.: Ice Prevention on Aircraft by Means of Engine Exhaust Heat and a Technical Study of Heat Transmission from a Clark Y Airfoil. Rep. No. 403, NACA, 1931.
4. Allen, H. Julian, and Look, Bonne C.: A Method for Calculating Heat Transfer in the Laminar Flow Region of Bodies. NACA R.B., Dec. 1942.
5. McAdams, William H.: Heat Transmission. McGraw-Hill Book Co., Inc., 1933.
6. Rodert, Lewis A., and Jackson, Richard: Preliminary Investigation and Design of an Air-Heated Wing for Lockheed 12A Airplane. NACA A.R.R., May 1942.

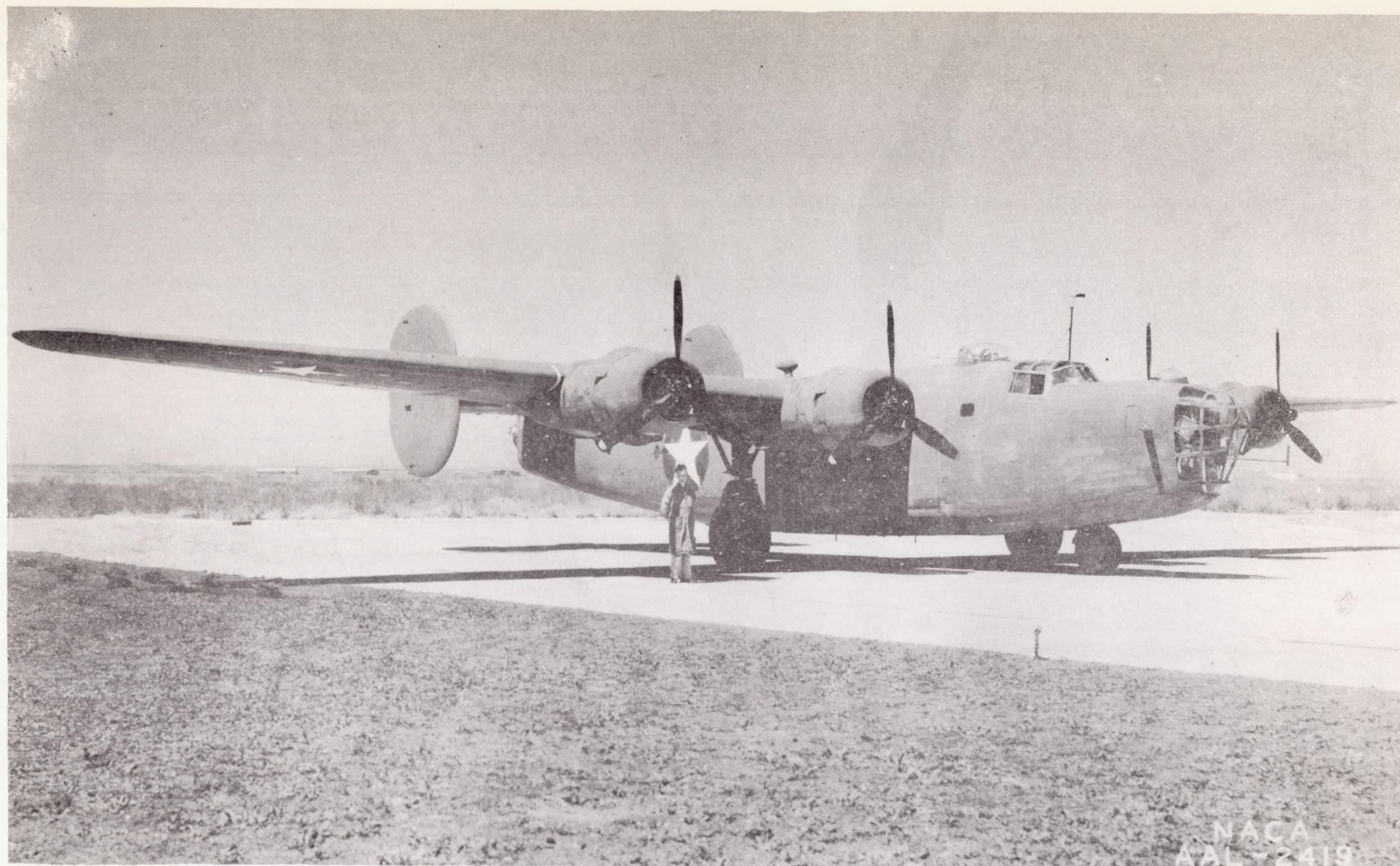


Figure 1.- The B-24D airplane in which thermal ice-prevention equipment on the wings, empennage, and windshields have been installed.

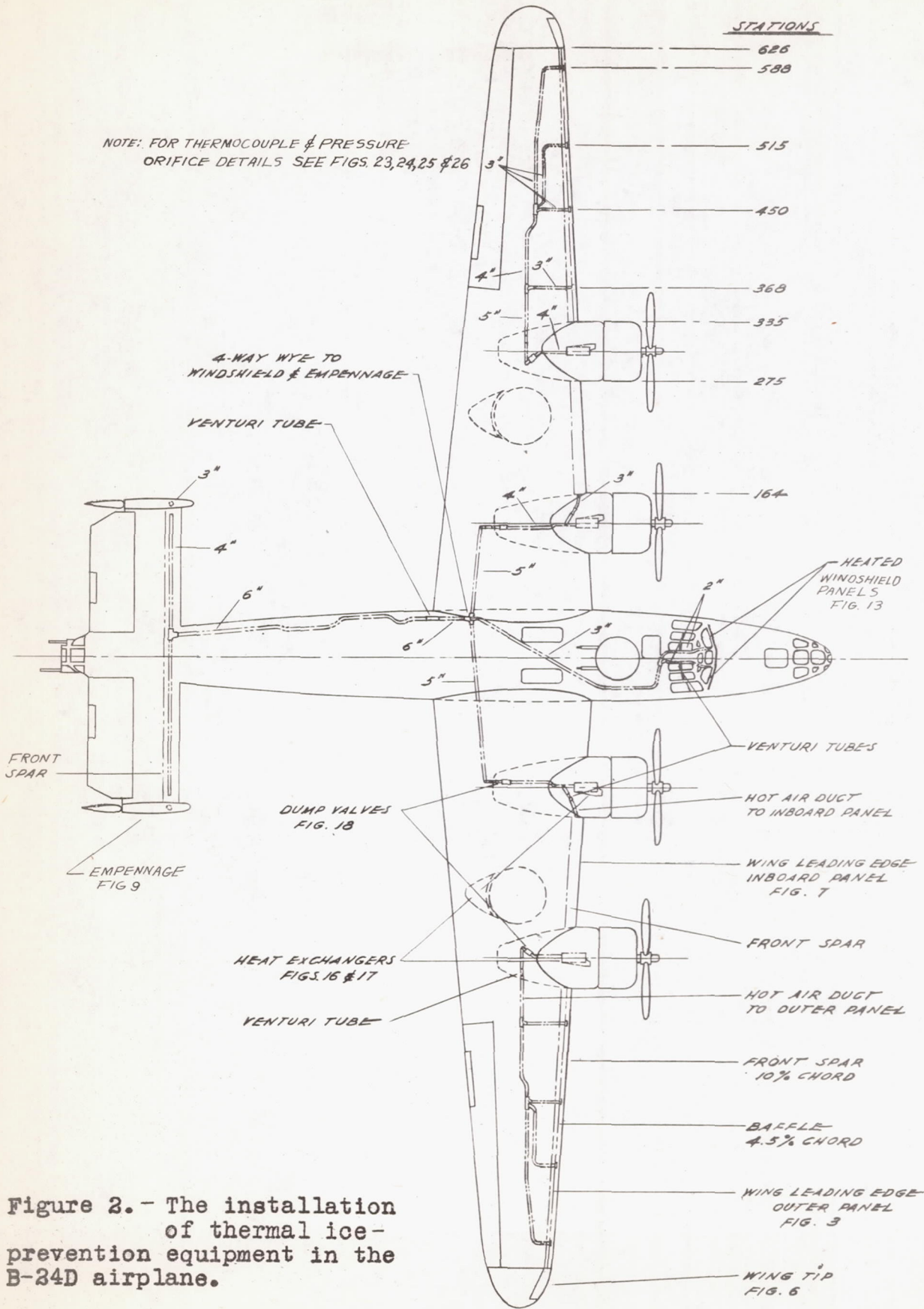


Figure 2.- The installation of thermal ice-prevention equipment in the B-24D airplane.

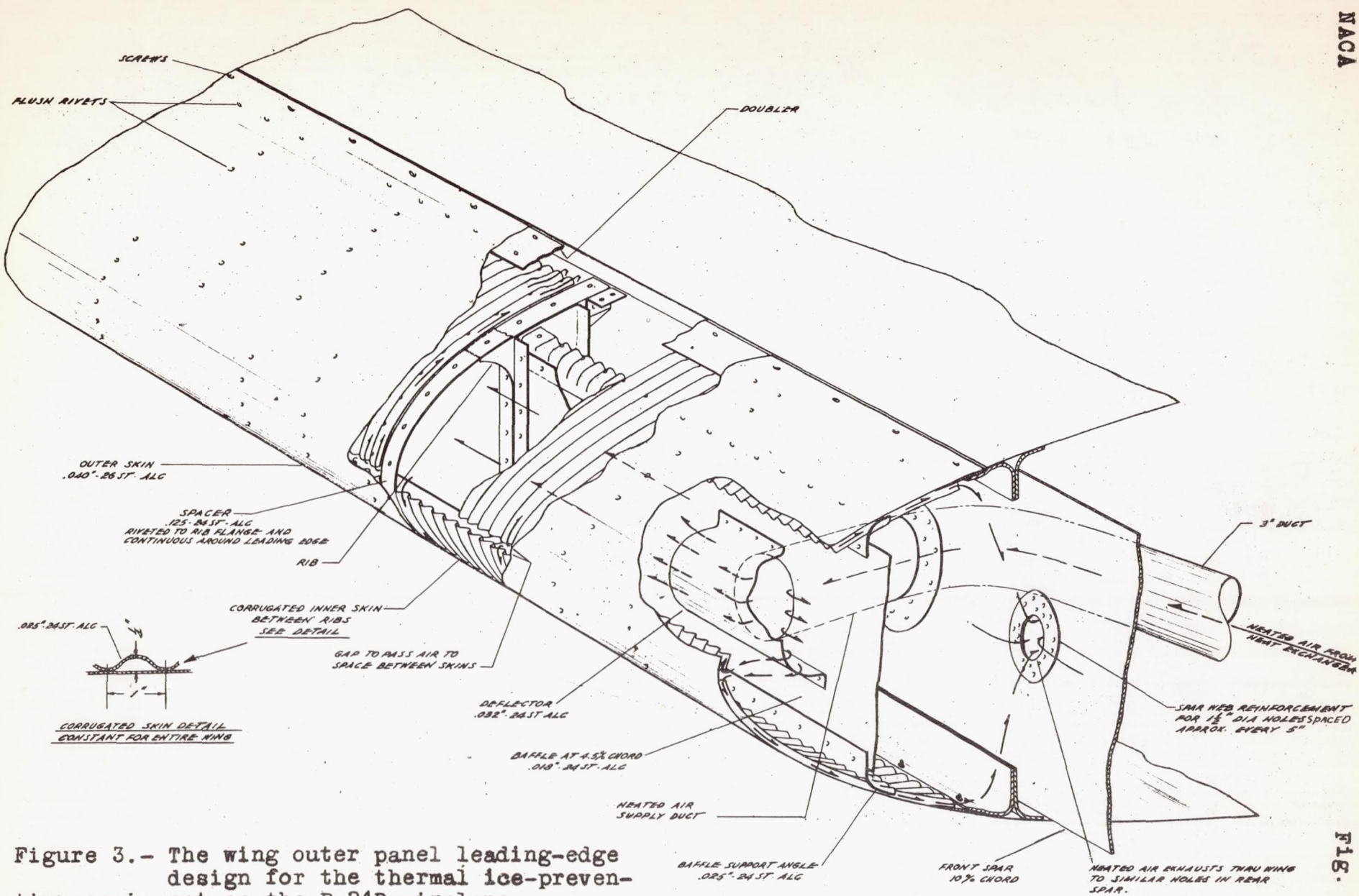


Figure 3.- The wing outer panel leading-edge design for the thermal ice-prevention equipment on the B-24D airplane.

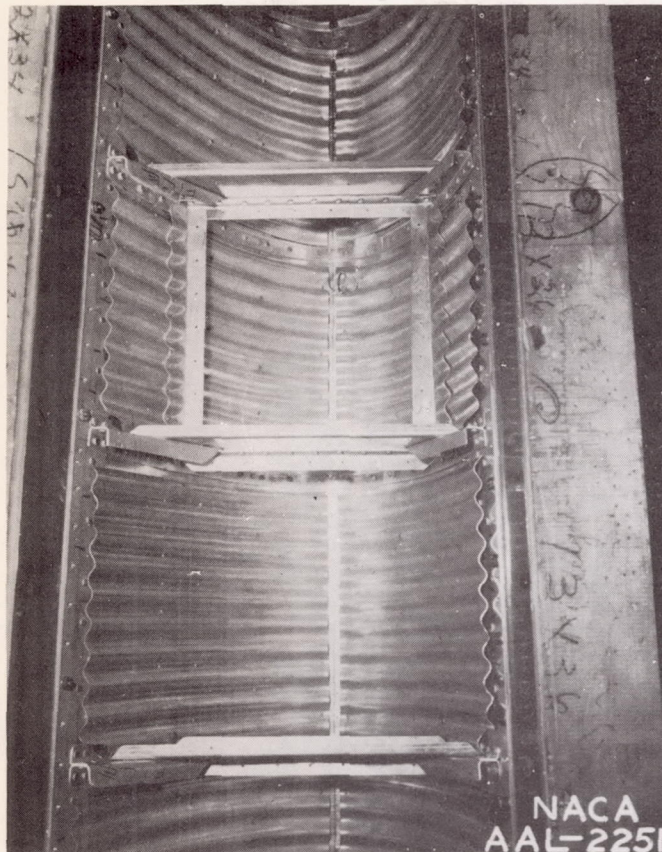
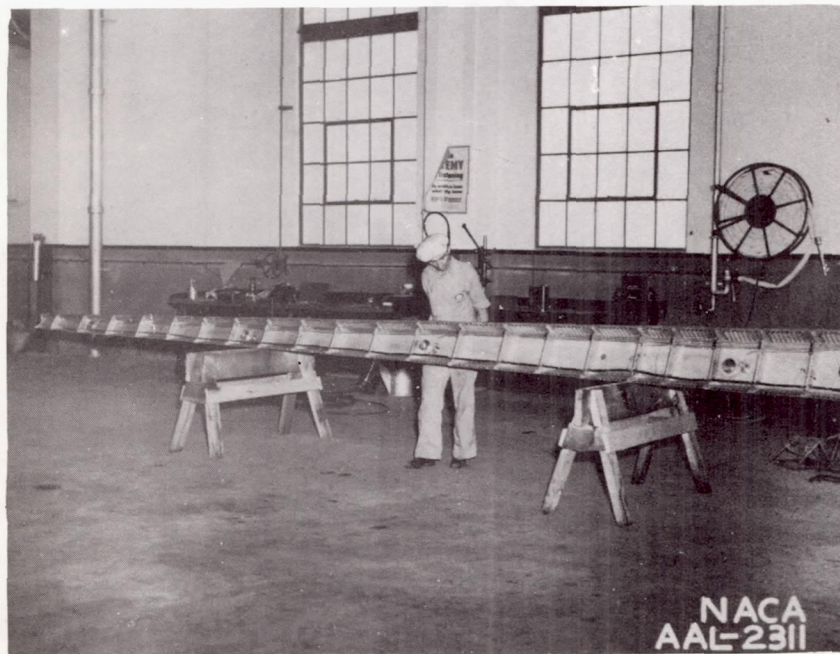


Figure 4.-
 Details of
 the wing
 outer panel
 leading
 edge of the
 B-24D air-
 plane during
 alteration
 for the
 thermal ice-
 prevention
 equipment.
 Shown are
 the air gap
 at the lead-
 ing edge,
 nose rib
 construction,
 and the baffle
 support angles.

Figure 5.-
 The right
 wing outer
 panel lead-
 ing edge
 for the B-24D
 airplane
 after the
 alterations
 were
 completed
 for the in-
 stallation
 of the
 thermal ice-
 prevention
 equipment.
 The photo-
 graph shows
 the heated-
 air supply
 inlet holes
 through the
 baffle plate.



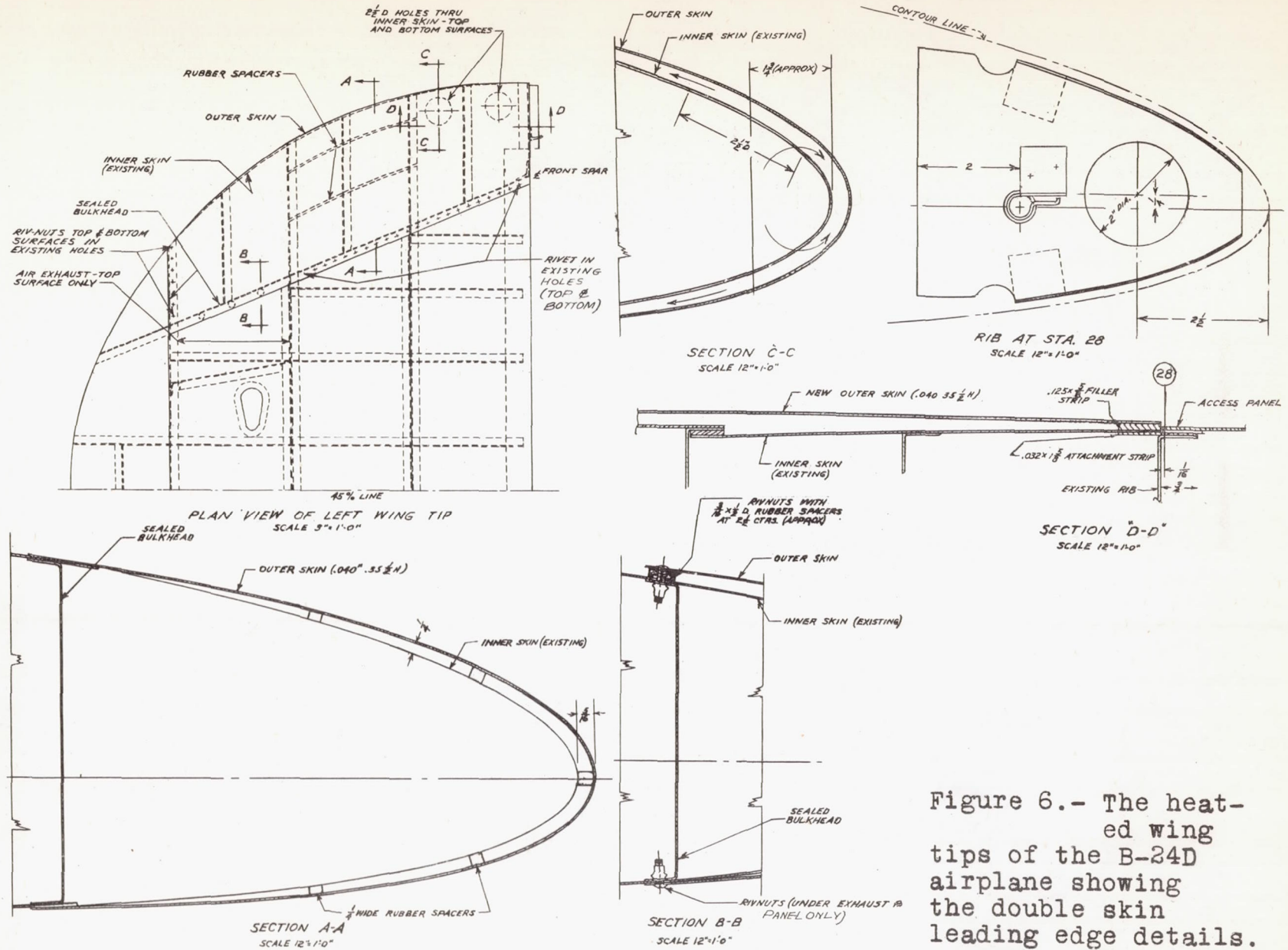


Figure 6.- The heat-ed wing tips of the B-24D airplane showing the double skin leading edge details.

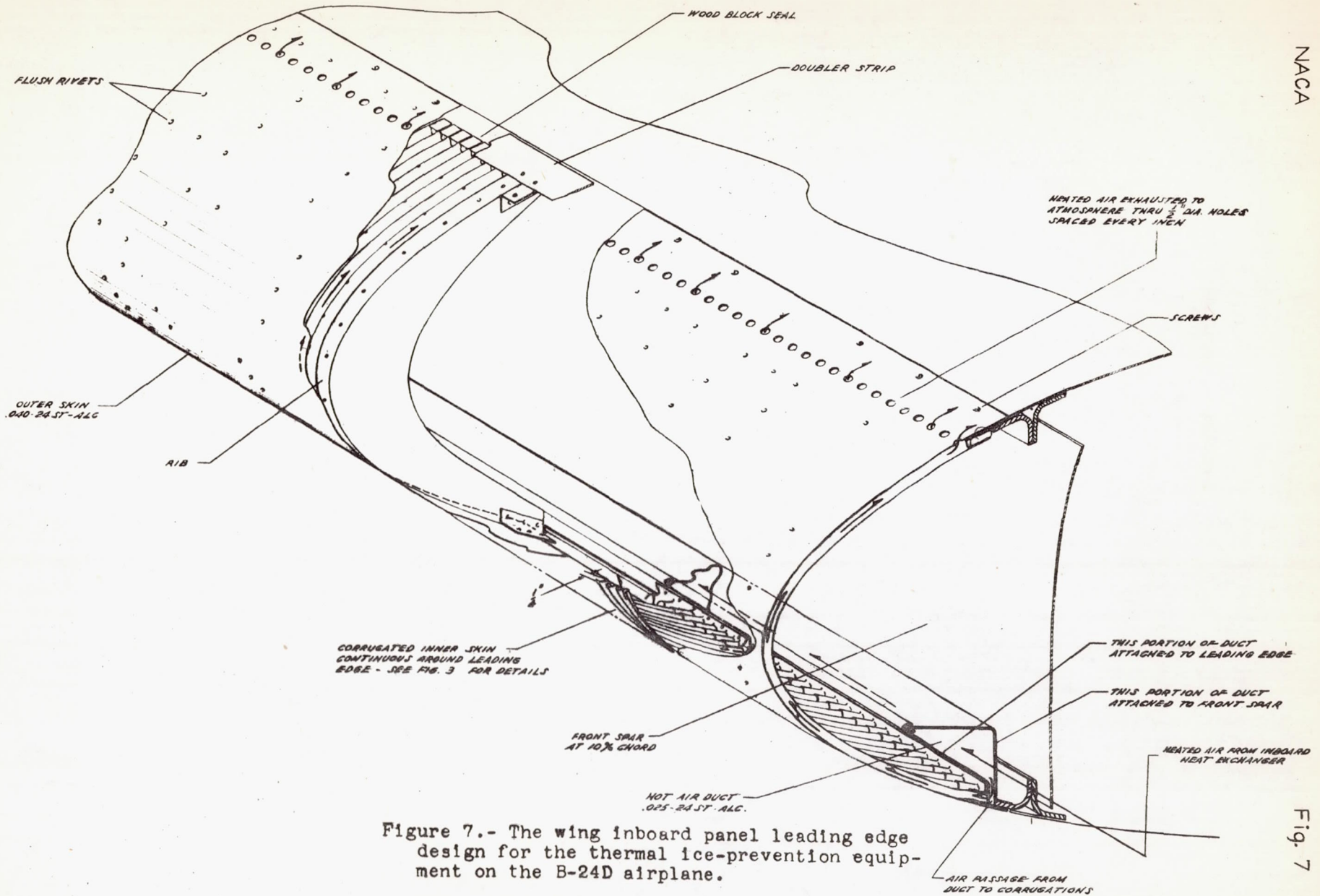


Figure 7.- The wing inboard panel leading edge design for the thermal ice-prevention equipment on the B-24D airplane.

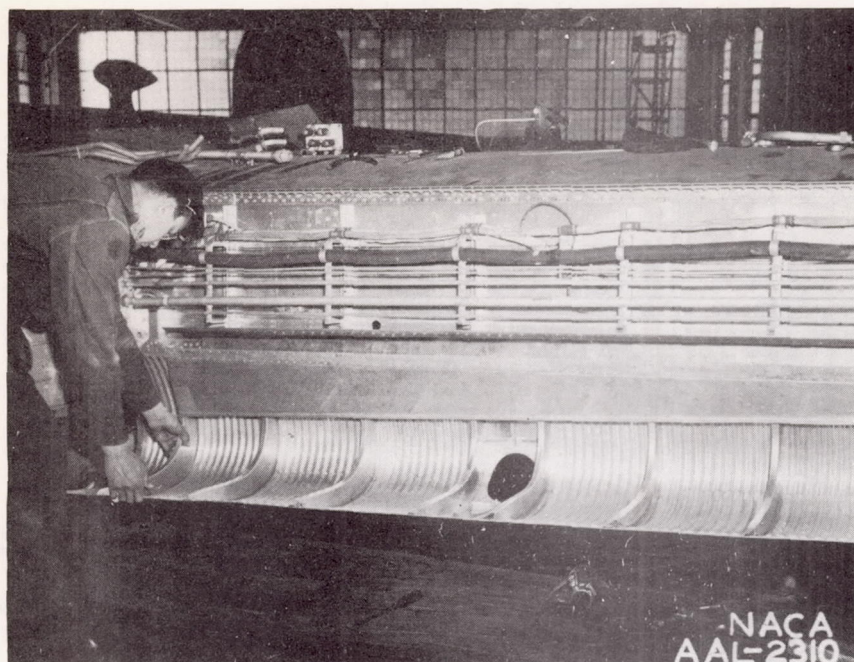


Figure 8.- The left wing inboard panel leading edge of the B-24D airplane shown during the installation of the thermal ice-prevention equipment.

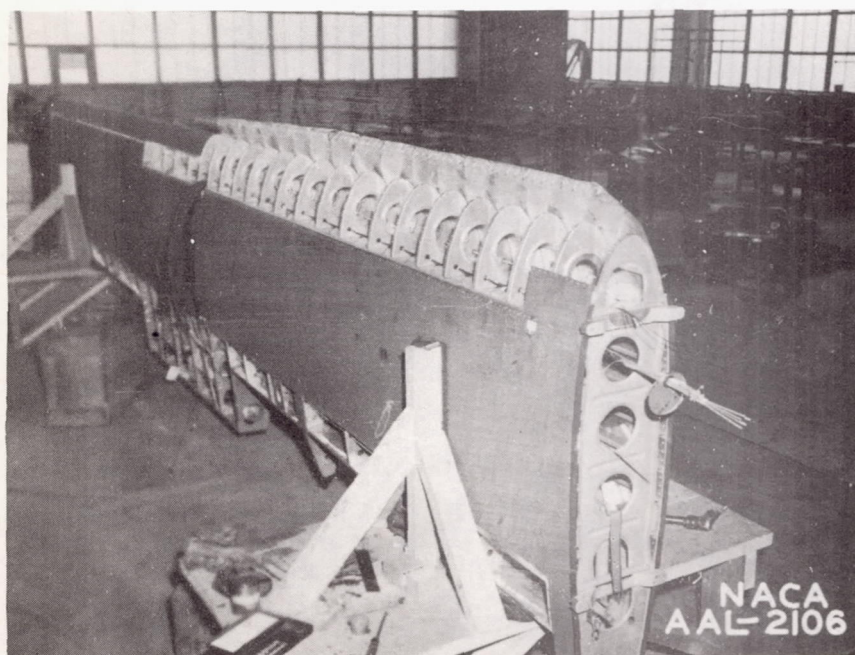


Figure 10.- The horizontal stabilizer of the B-24D airplane during the installation of thermal ice-prevention equipment, showing the lightening holes in the nose ribs through which the heated-air duct was installed. The stabilizer is viewed from above in this photograph.

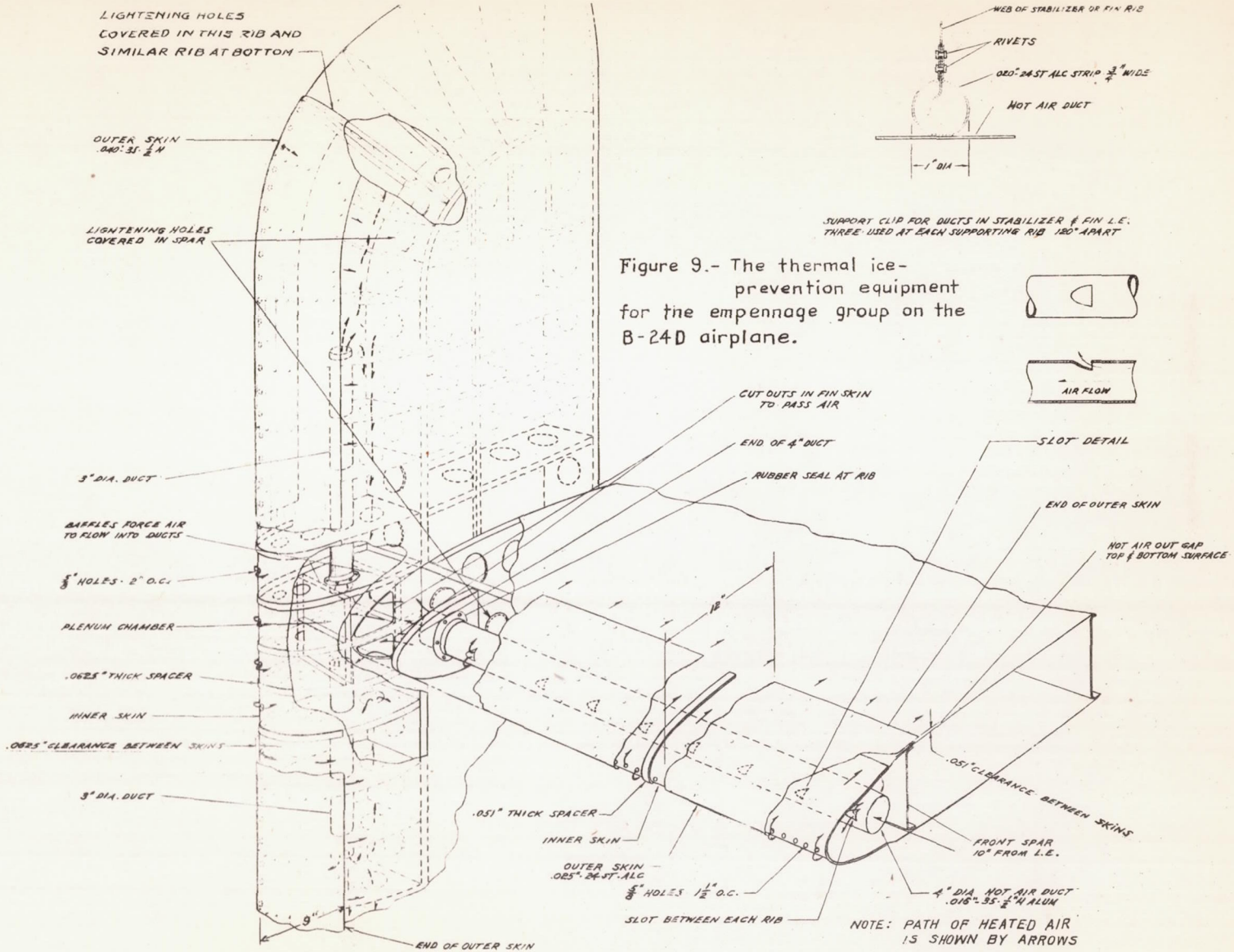


Figure 9.- The thermal ice-prevention equipment for the empennage group on the B-24D airplane.

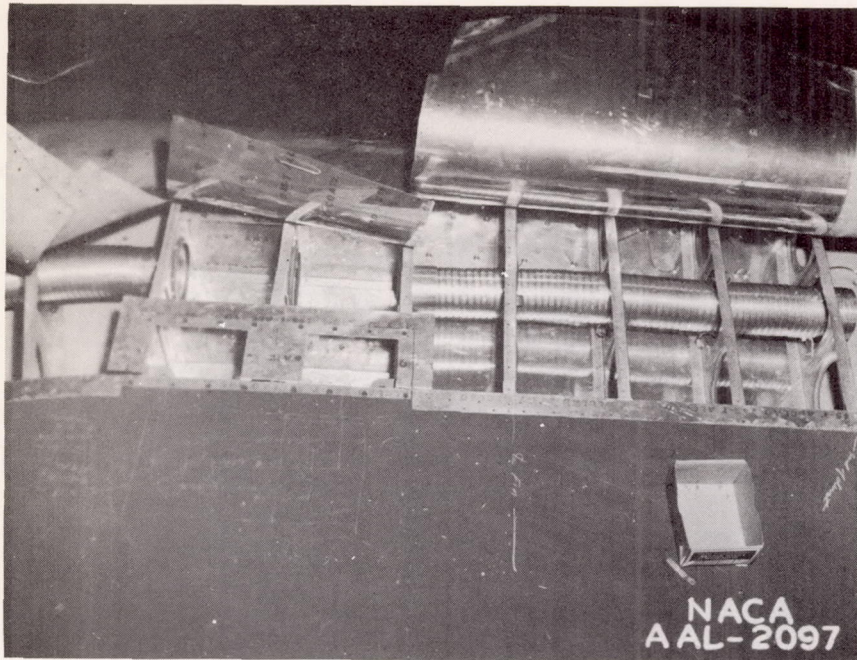


Figure 11.- The inboard side of the right vertical fin of the B-24D airplane during the installation of the thermal ice-prevention equipment, showing the plenum chamber and air ducts running to the top and bottom of the fin.

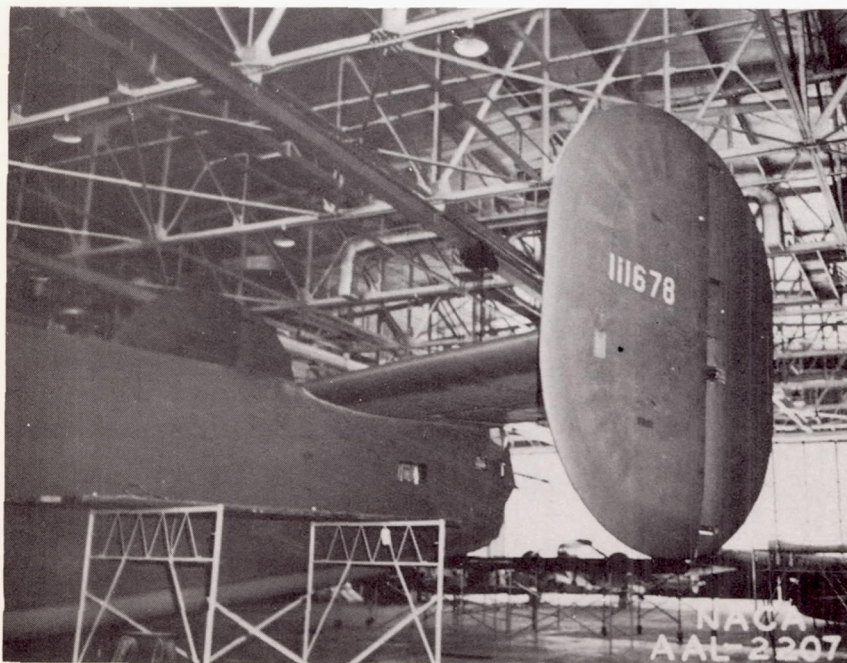
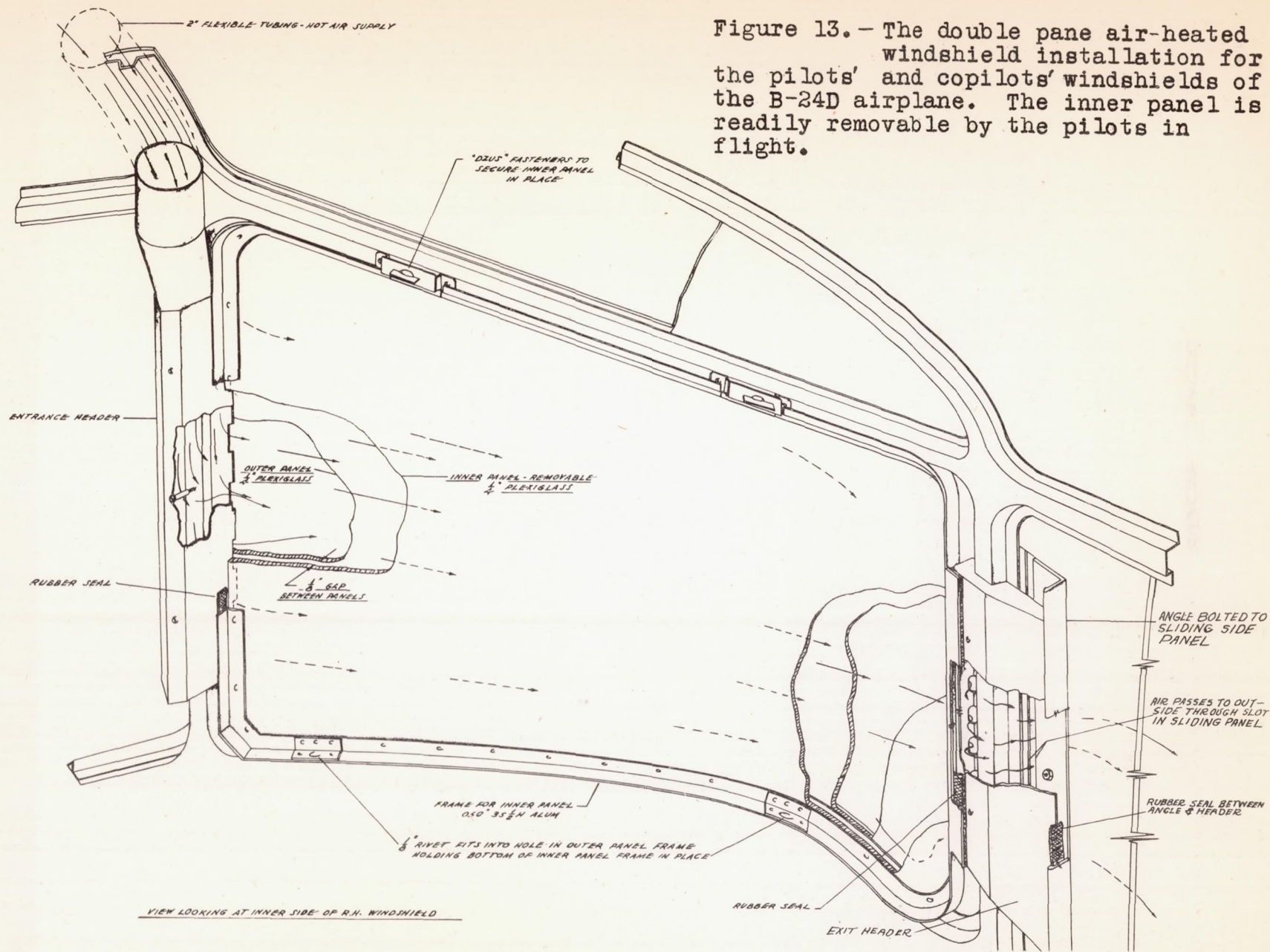


Figure 12.- The empennage group of the B-24D airplane in which provision has been made for thermal ice prevention.

Figure 13.- The double pane air-heated windshield installation for the pilots' and copilots' windshields of the B-24D airplane. The inner panel is readily removable by the pilots in flight.



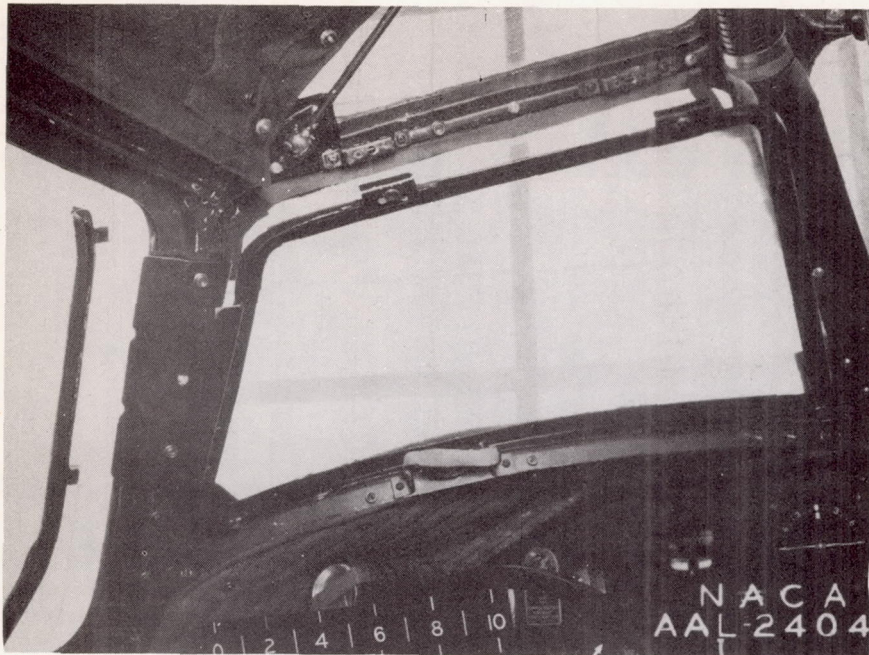


Figure 14.- The pilot's air-heated windshield on the B-24D airplane, showing the inner panel partially removed.

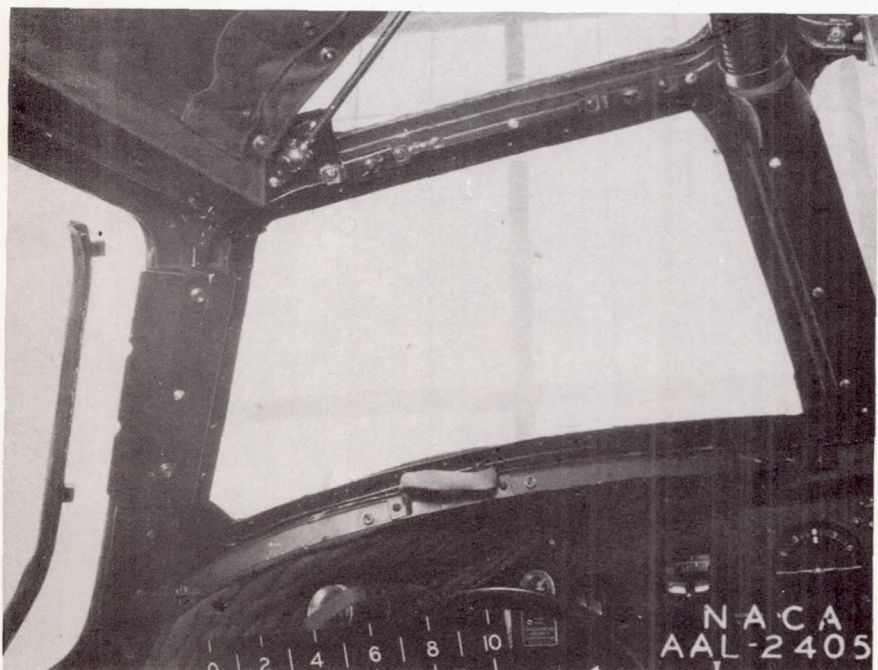


Figure 15.- The pilot's air-heated windshield on the B-24D airplane, with the inner panel secured in position.

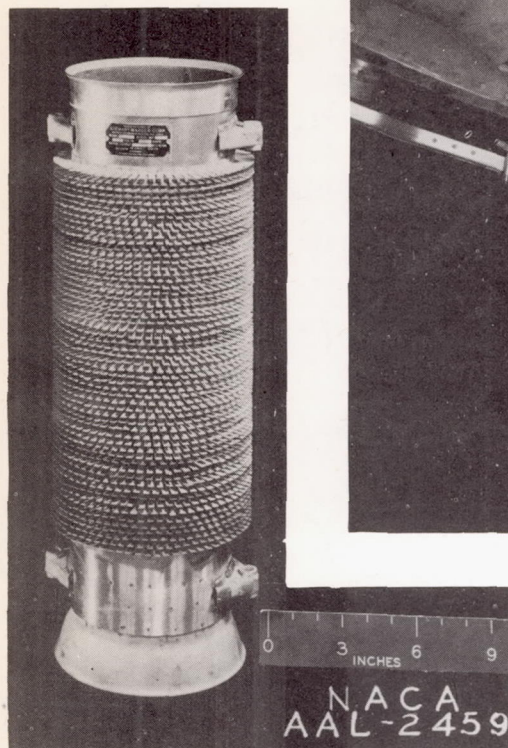


Figure 16.- A section of the B-24D airplane exhaust gas tail-stack which has been converted to a fin-type surface heat exchanger for use with the thermal ice-prevention equipment.

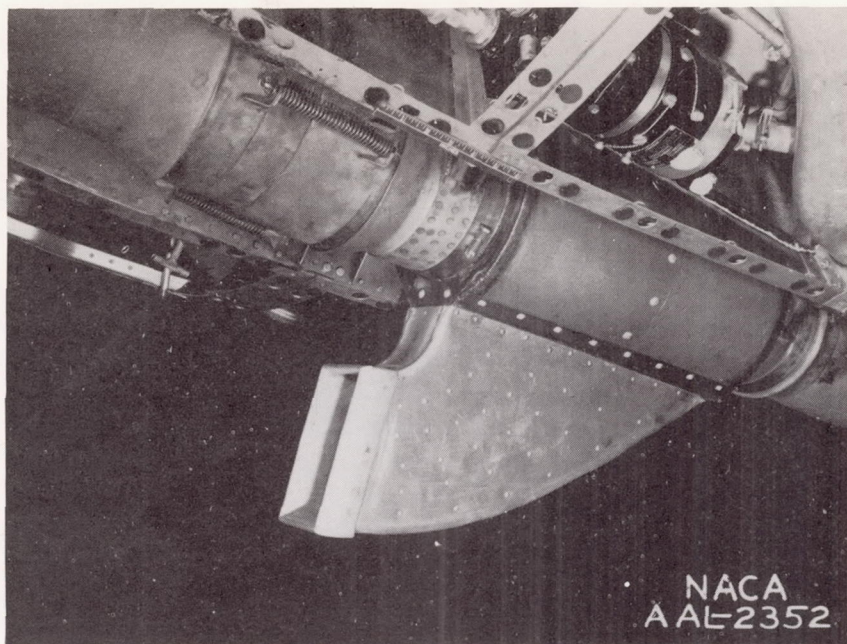
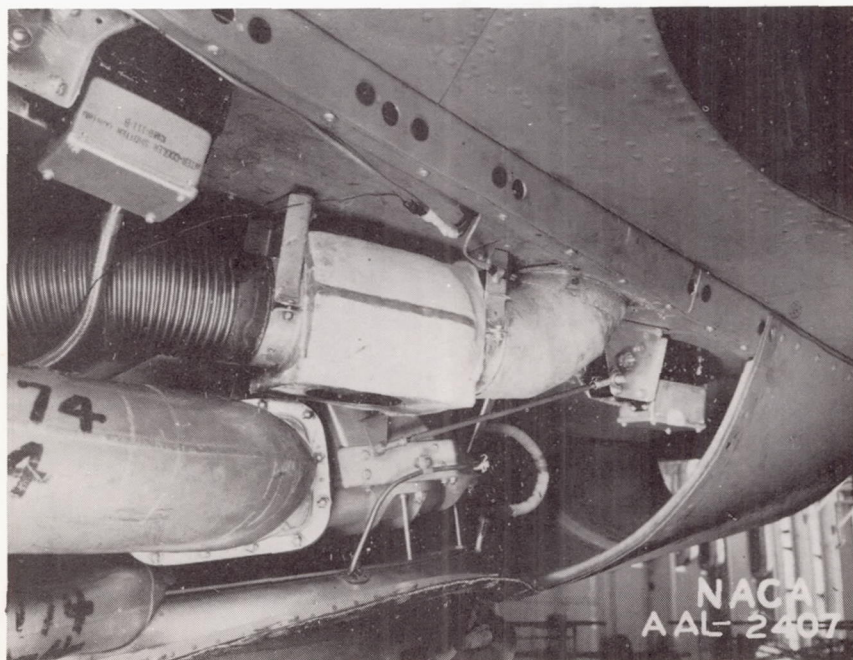


Figure 17.- The exhaust-air heat exchanger installation on the B-24D airplane in the right outboard nacelle.

Figure 18.- The heated-air dump valve for the right outboard exchanger on the B-24D airplane. The position of the electric motor-operated valve determines whether or not the heated air enters the thermal ice-prevention equipment.



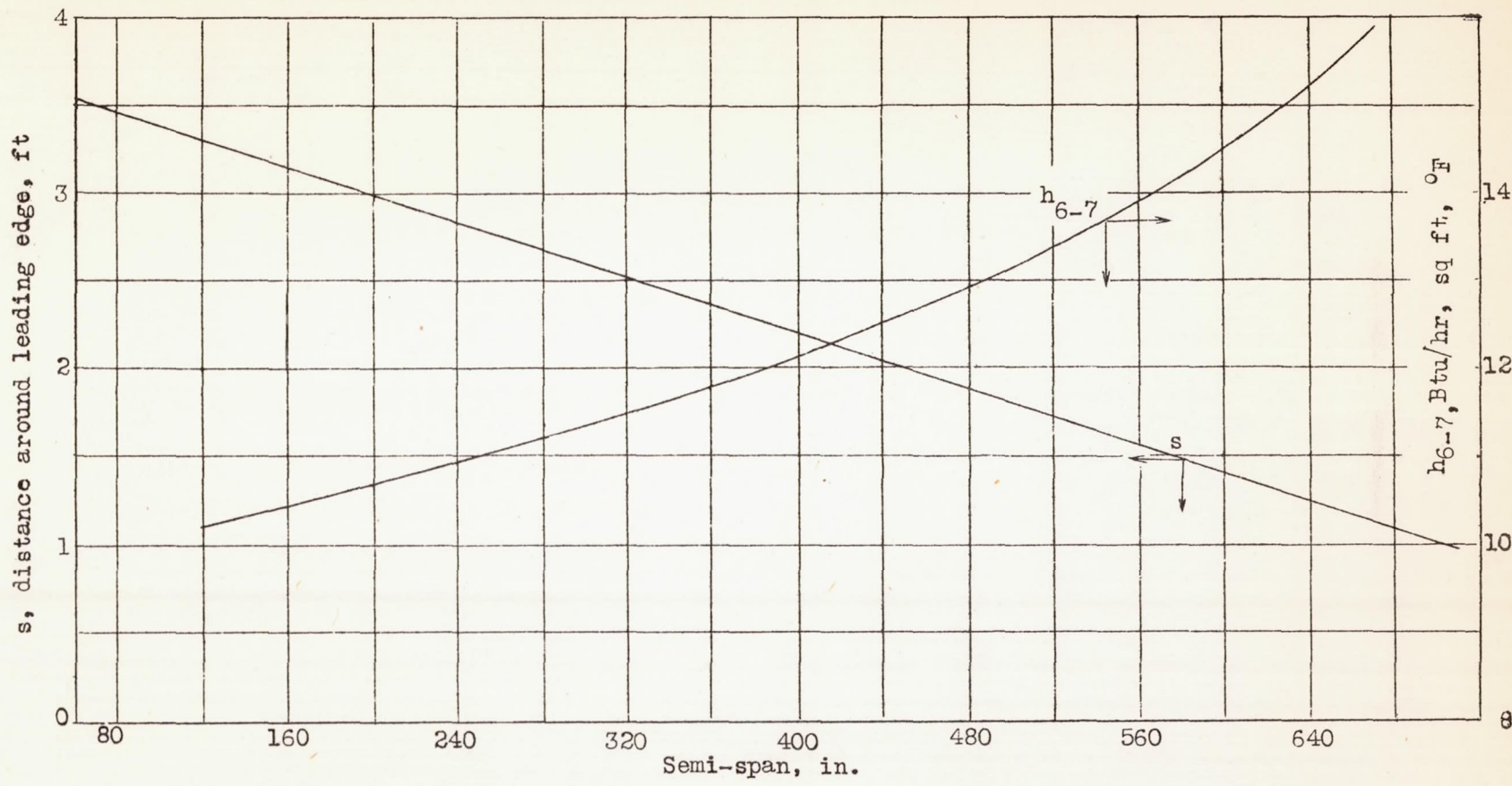


Figure 19.- Curves showing the distance around the leading edge from top to bottom of front spar, and the heat transfer coefficient, for the leading edge of the wing surface on the B-24D airplane.

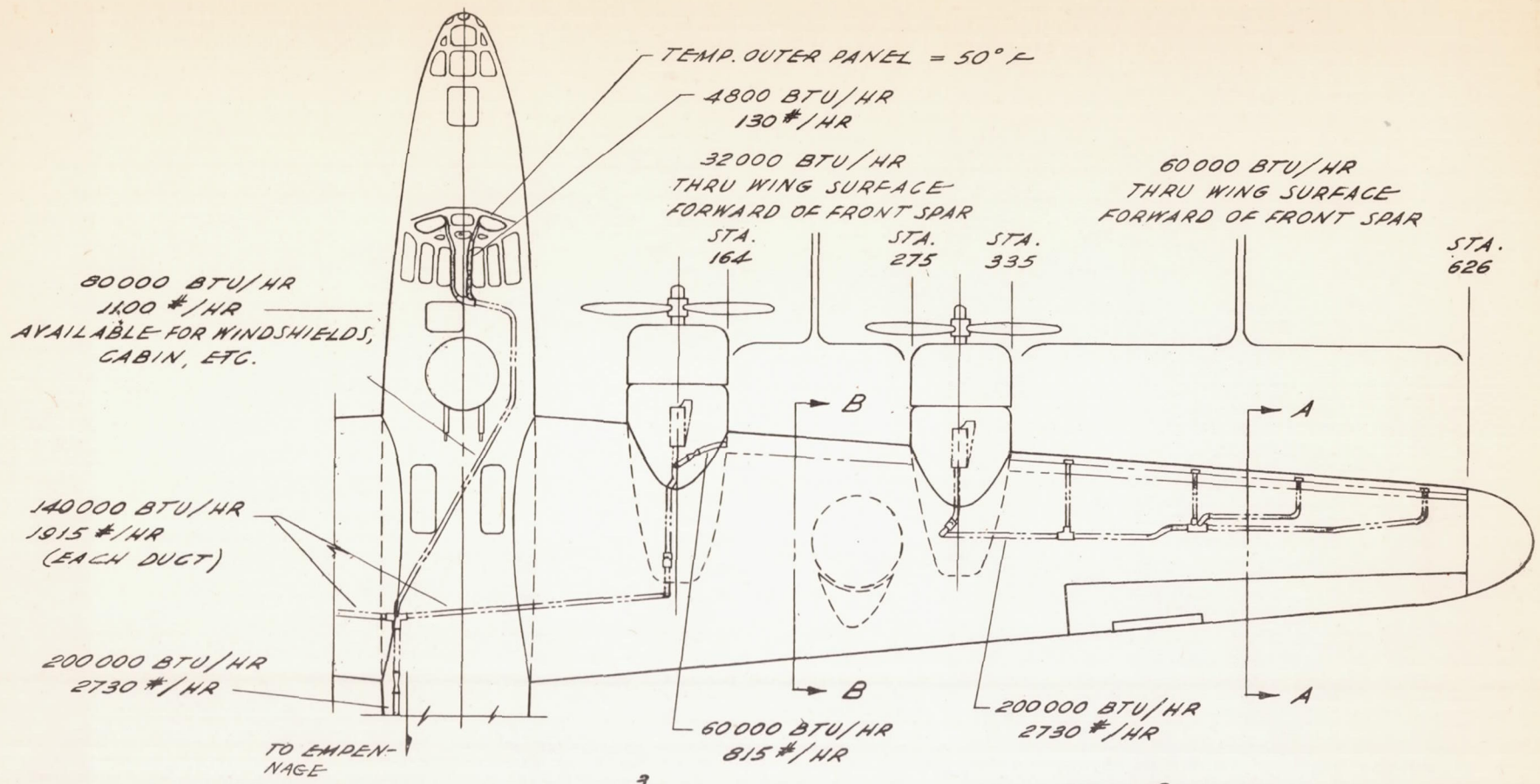
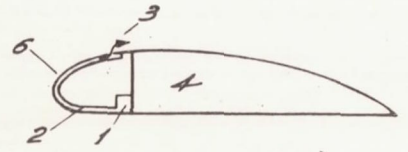


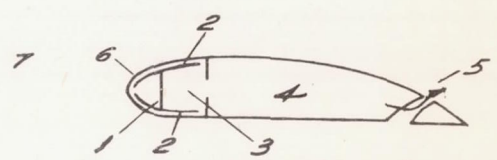
Figure 20.- The results of the analysis of the thermal ice-prevention equipment, showing the distribution of the heated air in the wings and windshield in the B-24D airplane.



$t_7 = 0^\circ F$
 $t_6 = 110^\circ F$
 $p_1 - p_3 = 5 \text{ IN. OF WATER}$

FOR ENTIRE INBOARD PANEL

SECT. "B-B"



$t_7 = 0^\circ F$
 $t_6 = 100^\circ F$
 $p_1 - p_3 = 0.6 \text{ IN. OF WATER}$

FOR ENTIRE OUTER PANEL

SECT. "A-A"

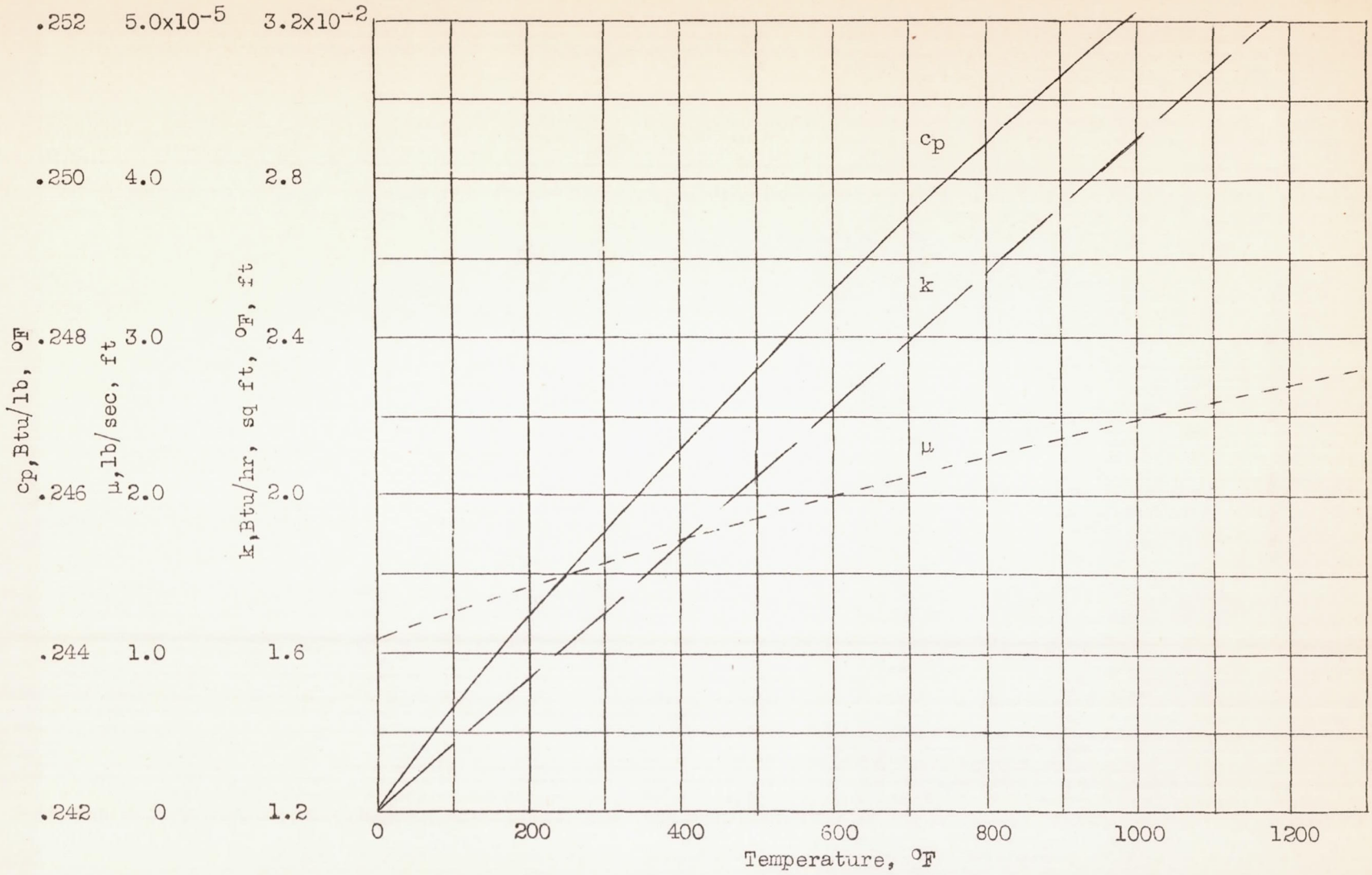
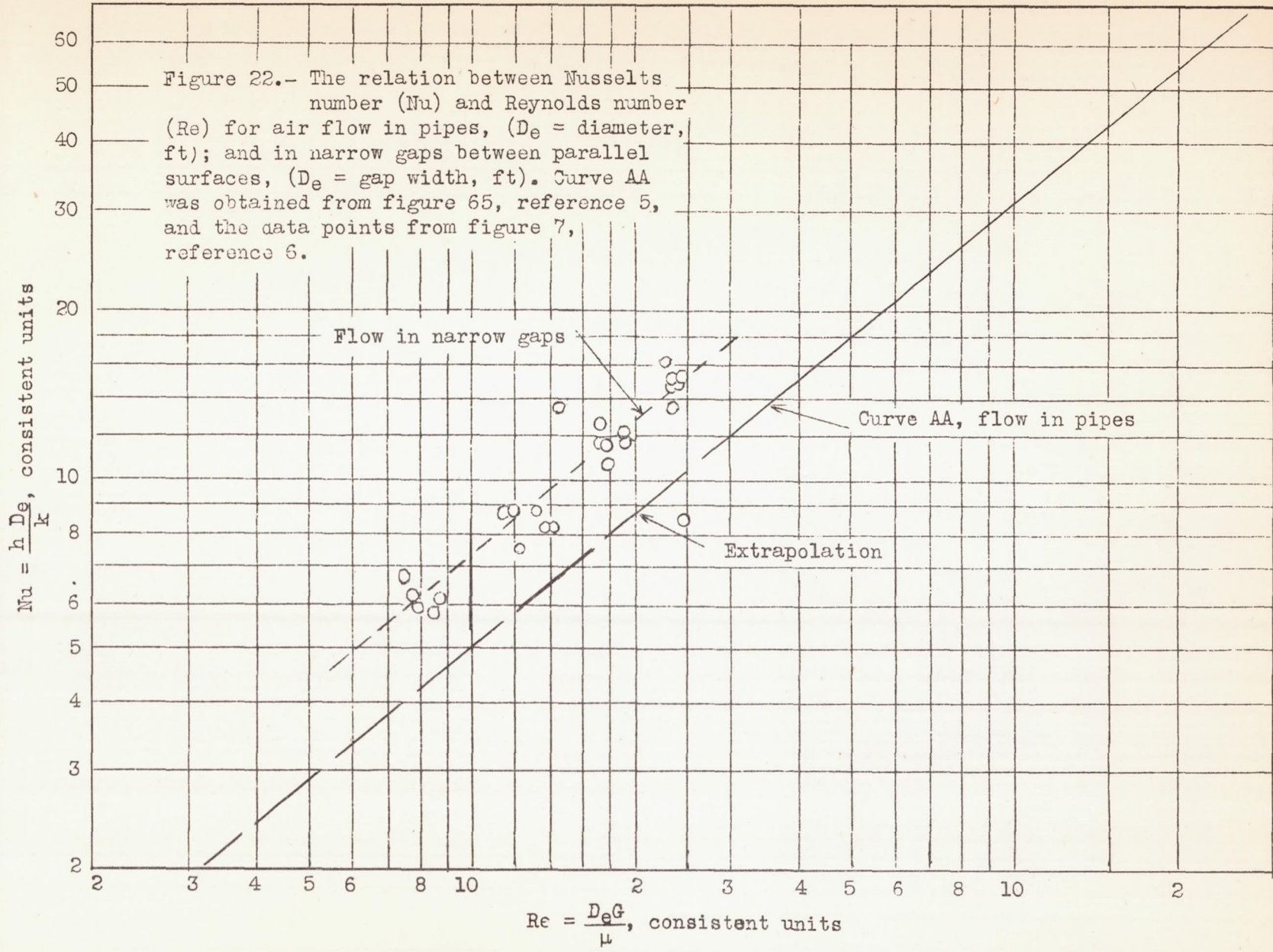
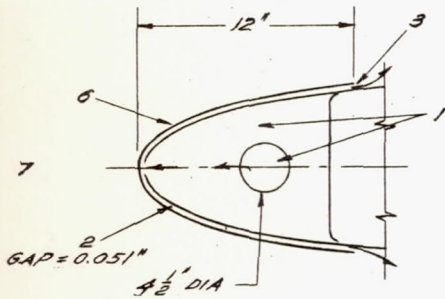
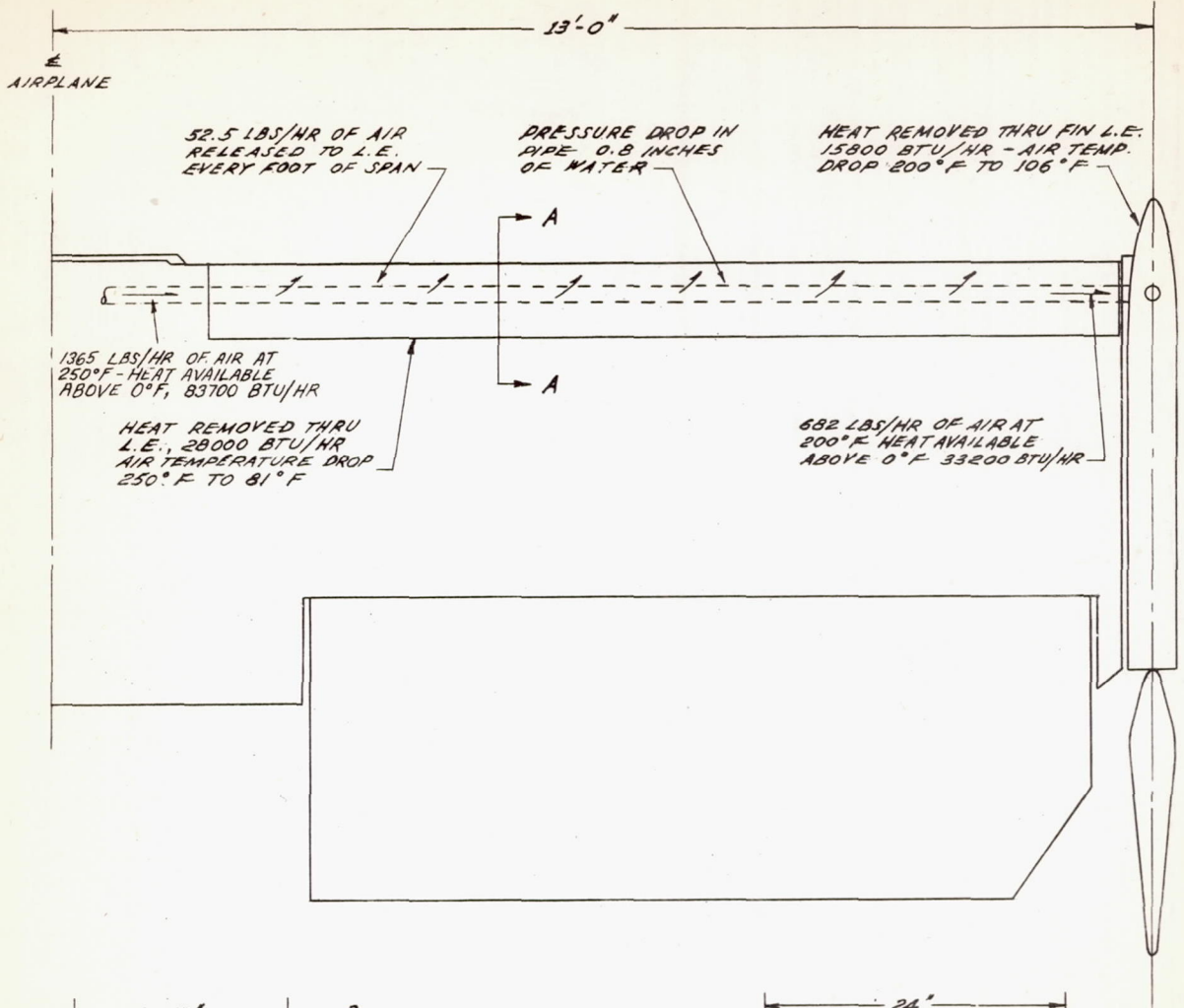


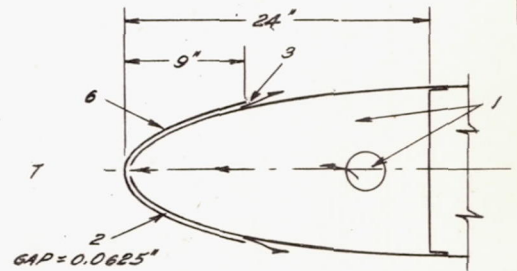
Figure 21.- The physical properties of air as employed in the analysis of the thermal ice-prevention equipment.





$t_6 = 90^\circ F$
 $P_1 - P_3 = 3.8 \text{ IN. OF WATER}$

SECTION "A-A"
 CONSTANT ALONG SPAN



$t_6 = 70^\circ F$
 $P_1 - P_3 = 2.1 \text{ IN. OF WATER}$

SECTION THRU FIN
 CONSTANT ALONG LEADING EDGE

Figure 23.- The results of the analysis of the thermal ice-prevention equipment, showing the distribution of the heated air in the empennage in the B-24D airplane.

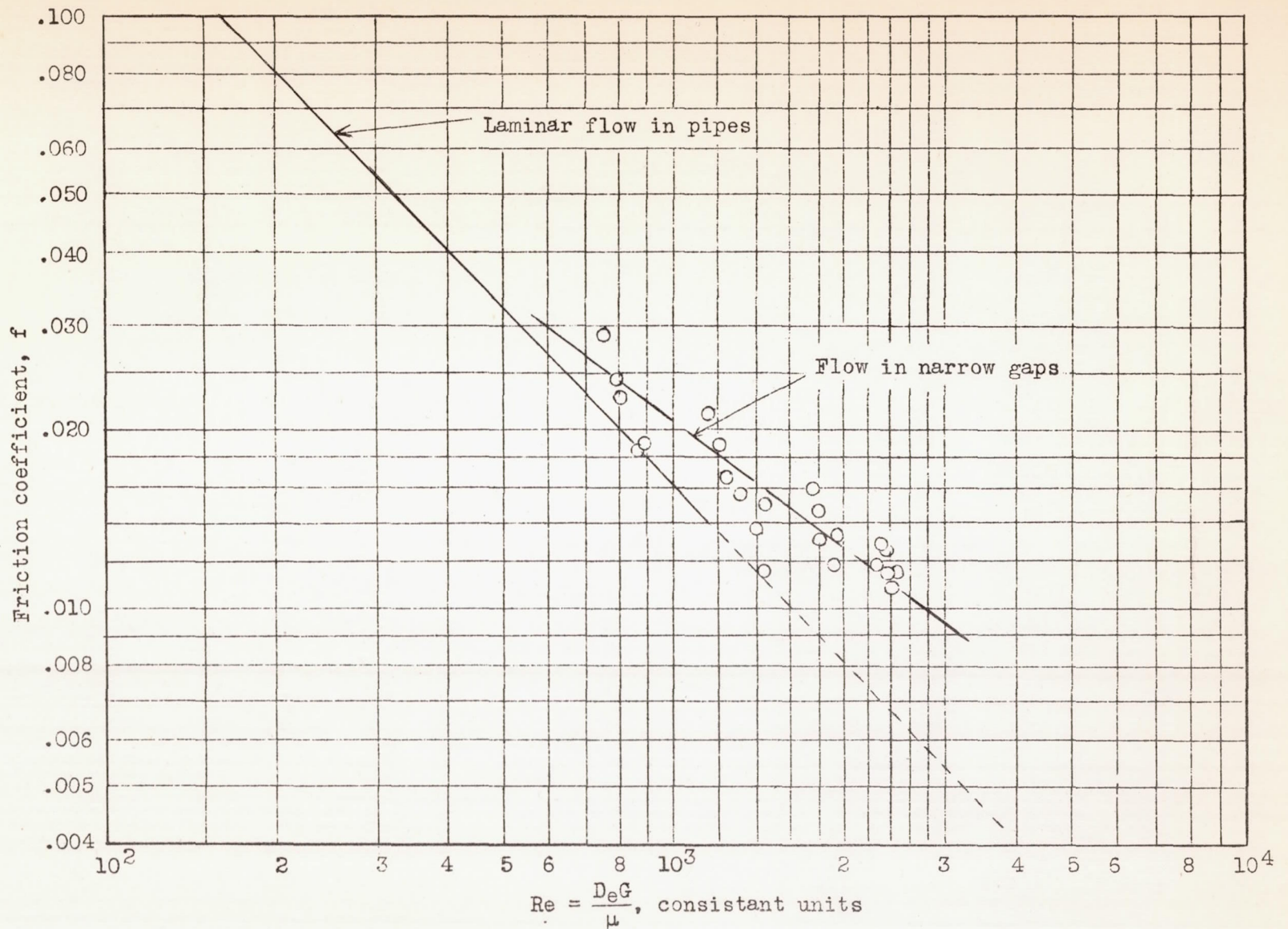


Figure 24.- The relation between the friction factor and Reynolds number for flow of air in pipes, (D_e = diameter, ft); and in narrow gaps between parallel surfaces, (D_e = gap width, ft) Taken from figure 8, reference 5.

NOTES & LEGEND

- A - AIR THERMOCOUPLES
- S - SKIN THERMOCOUPLES
- M - STRUCTURE THERMOCOUPLES
- G - EXHAUST GAS THERMOCOUPLES
- - ALL THERMOCOUPLES EXCEPT WING OR STABILIZER BOTTOM SURFACE & FIN OUTBOARD
- + - WING OR STABILIZER BOTTOM SURFACE OR FIN OUTBOARD

DASH NUMBERS FOLLOWING THERMOCOUPLE NUMBERS INDICATE TYPE OF THERMOCOUPLE MOUNTING AS DETAILED IN FIG. 26

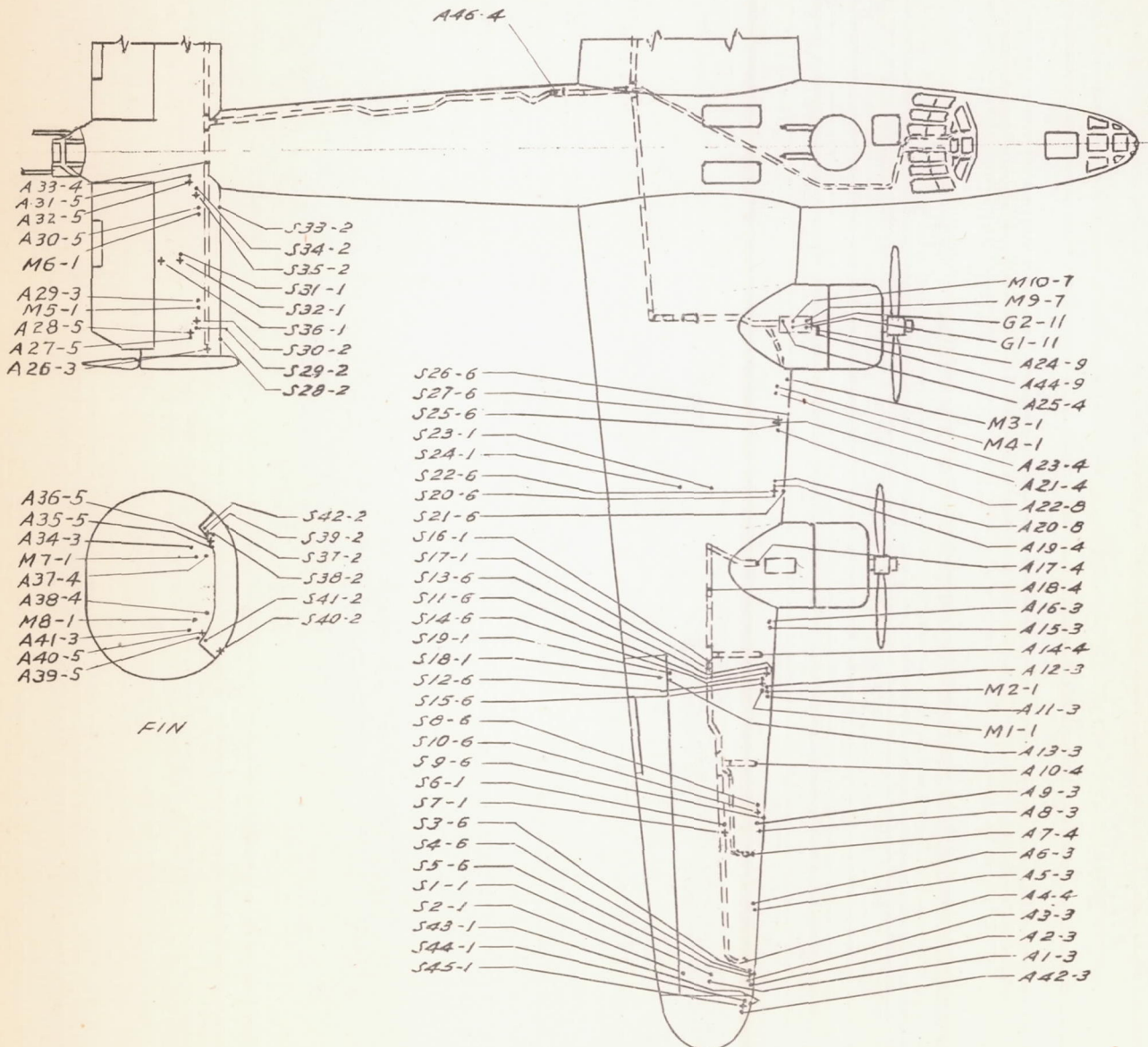
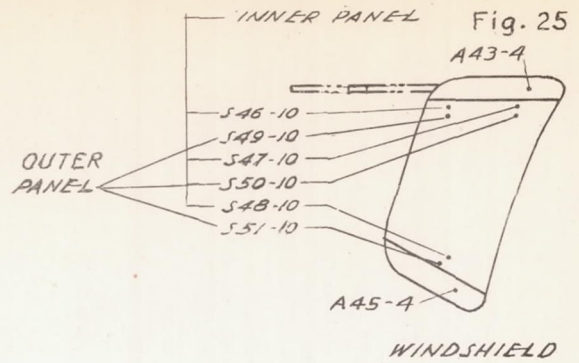


Figure 25.- The thermocouples which were installed on the B-24D airplane and which were employed in studying the thermal qualities of the ice-prevention equipment.

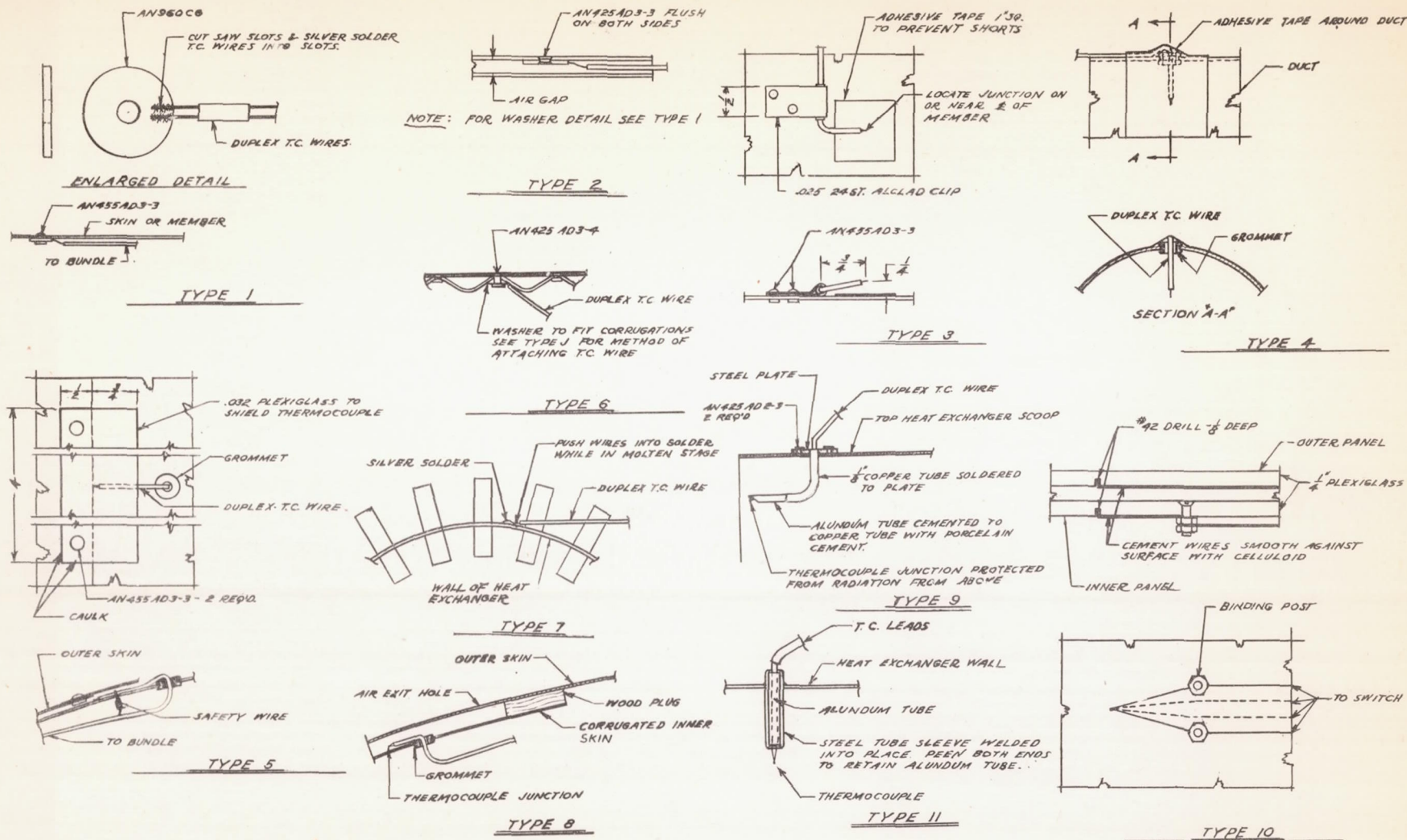


Figure 26.- Thermocouple installation details employed in the B-24D airplane thermal ice-prevention equipment.

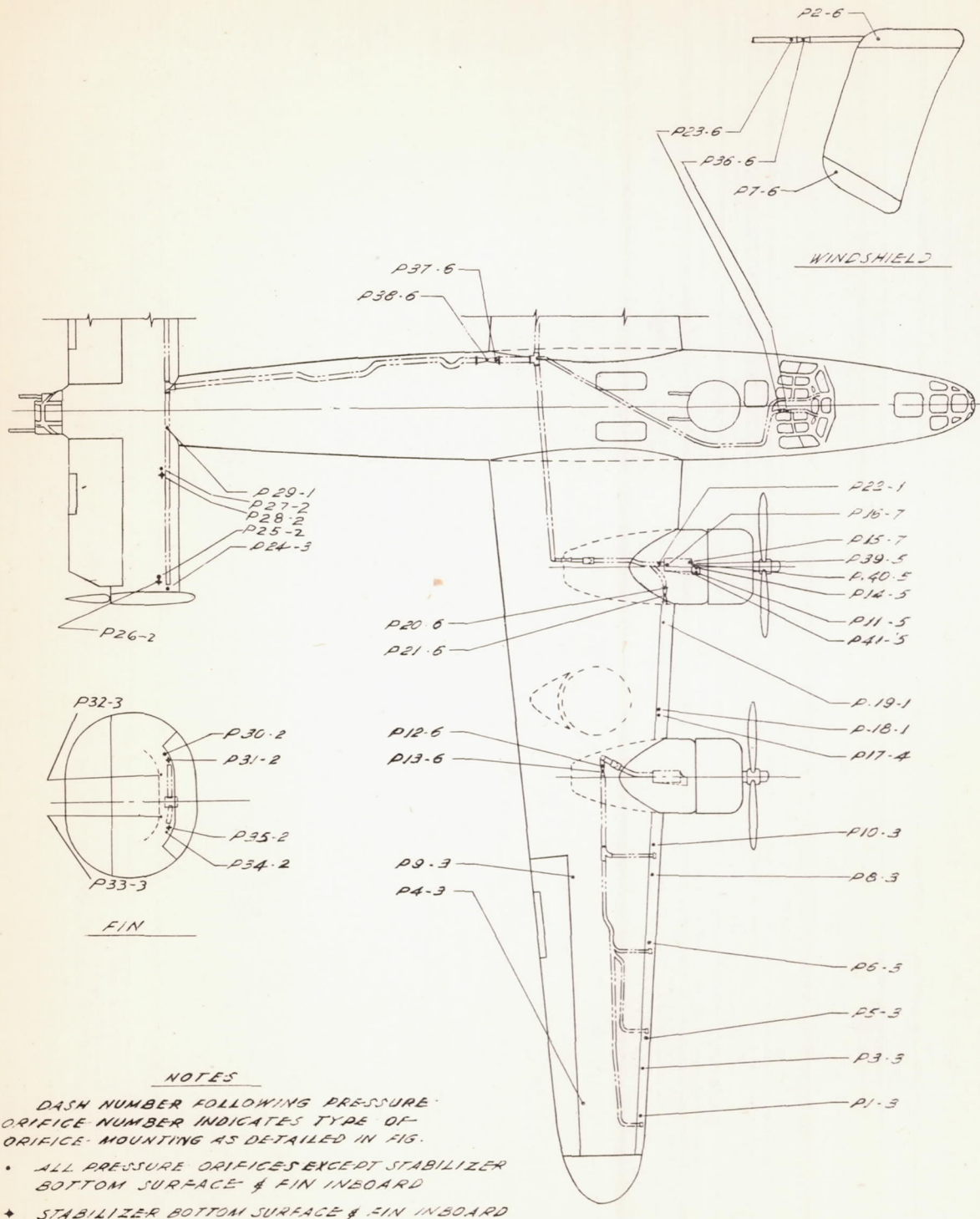
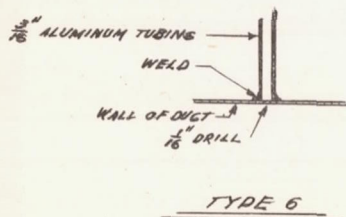
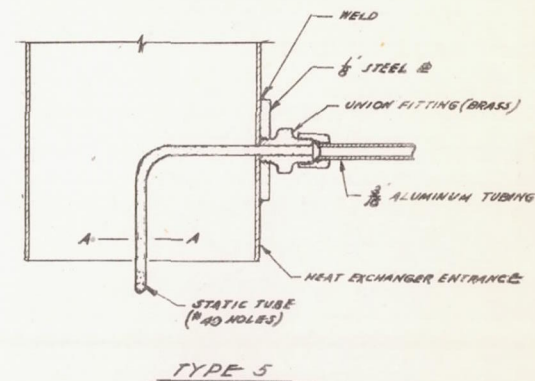
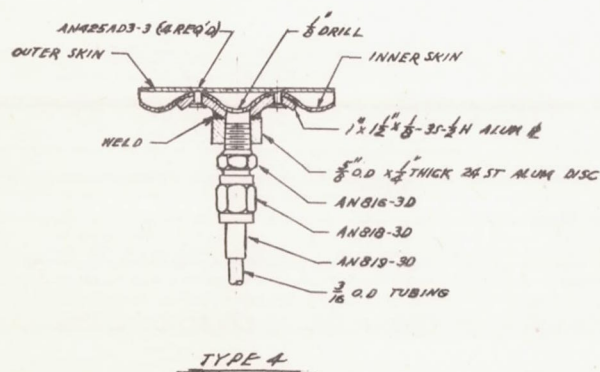
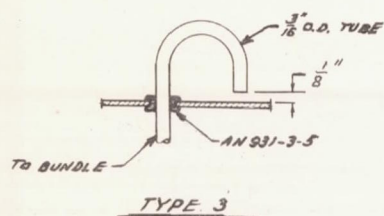
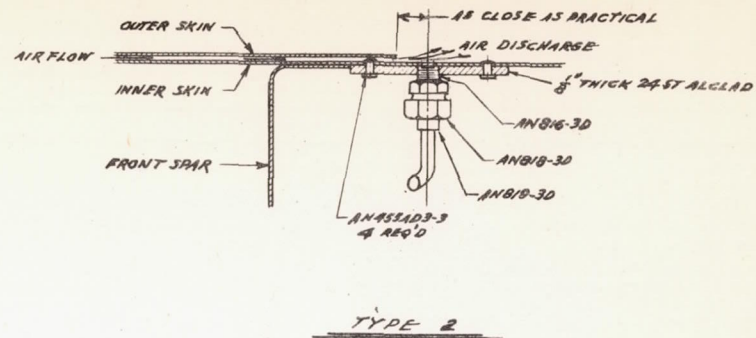
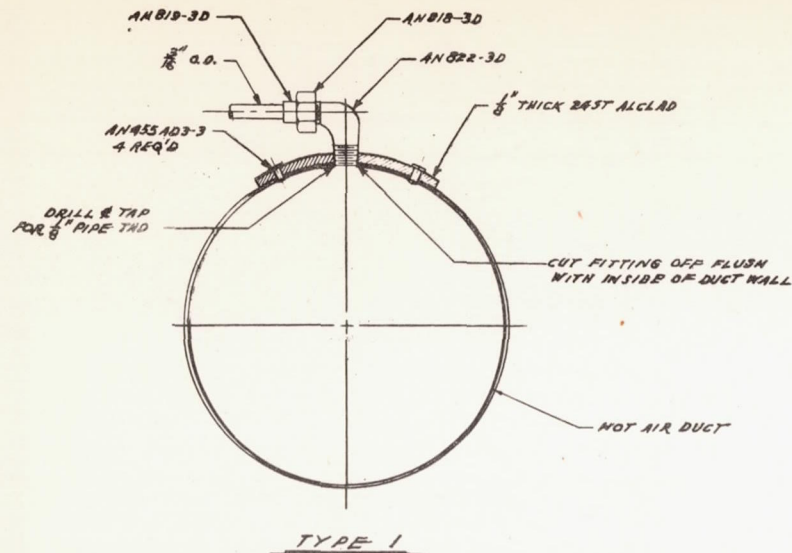


Figure 27.- The pressure orifices which were installed on the B-24D airplane and which were employed in studying the thermal qualities of the ice-prevention equipment.

A-35



NOTE: TOTAL PRESSURE TUBE HAS IDENTICAL MOUNTING, WITH TUBE CUT OFF SQUARE AT "A-A" AND LOCATED 3" BELOW STATIC TUBE

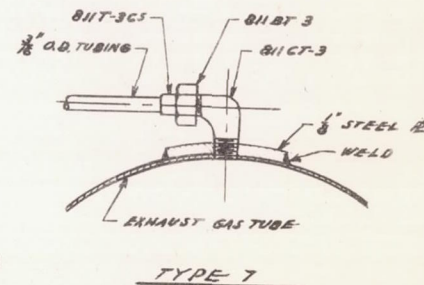


Figure 28.- Pressure orifice details employed in the B-24D airplane thermal ice-prevention equipment.